

Genotyping-by-sequencing and microarrays are complementary for detecting quantitative trait loci by tagging different haplotypes in association studies

Sandra Silvia Negro, Emilie Millet, Delphine Madur, Cyril Bauland, Valerie Combes, Claude Welcker, Francois Tardieu, Alain Charcosset, Stephane S.

Nicolas

▶ To cite this version:

Sandra Silvia Negro, Emilie Millet, Delphine Madur, Cyril Bauland, Valerie Combes, et al.. Genotyping-by-sequencing and microarrays are complementary for detecting quantitative trait loci by tagging different haplotypes in association studies. 2018. hal-02786986

HAL Id: hal-02786986 https://hal.inrae.fr/hal-02786986

Preprint submitted on 5 Jun 2020

HAL is a multi-disciplinary open access archive for the deposit and dissemination of scientific research documents, whether they are published or not. The documents may come from teaching and research institutions in France or abroad, or from public or private research centers.

L'archive ouverte pluridisciplinaire **HAL**, est destinée au dépôt et à la diffusion de documents scientifiques de niveau recherche, publiés ou non, émanant des établissements d'enseignement et de recherche français ou étrangers, des laboratoires publics ou privés.



Distributed under a Creative Commons Attribution - NonCommercial - NoDerivatives 4.0 International License

| 1 | Genotyping-by-sequencing and microarrays are complementary for detecting |
|----|--|
| 2 | quantitative trait loci by tagging different haplotypes in association studies |
| 3 | |
| 4 | Sandra Silvia Negro ^{1,3} , Emilie Millet ^{2,4} , Delphine Madur ¹ , Cyril Bauland ¹ , Valérie Combes ¹ , |
| 5 | Claude Welcker ² , François Tardieu ² , Alain Charcosset ¹ , Stéphane Dimitri Nicolas ¹ |
| 6 | |
| 7 | Affiliations : |
| 8 | ¹ GQE – Le Moulon, INRA, Univ. Paris-Sud, CNRS, AgroParisTech, Université Paris-Saclay, |
| 9 | 91190 Gif-sur-Yvette, France. |
| 10 | ² Laboratoire d'Ecophysiologie des Plantes sous Stress Environnementaux (LEPSE), |
| 11 | UMR759, INRA-SupAgro, 34060 Montpellier, France. |
| 12 | ³ Present address: GIGA-R Medical Genomics, University of Liège, Belgium. |
| 13 | ⁴ Present address: Biometris, Department of Plant Science, Wageningen University & |
| 14 | Research, 6700 AA Wageningen, The Netherlands. |
| 15 | |
| 16 | E-mail addresses: |
| 17 | snegro@uliege.be; emilie.millet@wur.nl; delphine.madur@inra.fr; cyril.bauland@inra.fr; |
| 18 | valerie.combes@inra.fr; claude.welcker@inra.fr; francois.tardieu@inra.fr; |
| 19 | alain.charcosset@inra.fr; stephane.nicolas@inra.fr |
| 20 | Corresponding author: |
| 21 | stephane.nicolas@inra.fr |

22

23 Abstract

24 Background: Single Nucleotide Polymorphism (SNP) array and re-sequencing technologies 25 have different properties (e.g. calling rate, minor allele frequency profile) and drawback (e.g. 26 ascertainment bias), which lead us to study the complementarity and consequences of using 27 them separately or combined in diversity analyses and Genome-Wide Association Studies 28 (GWAS). We performed GWAS on three traits (grain yield, plant height and male flowering 29 time) measured in 22 environments on a panel of 247 diverse dent maize inbred lines using 30 three genotyping technologies (Genotyping-By-Sequencing, Illumina Infinium 50K and 31 Affymetrix Axiom 600K arrays).

32 **Results:** The effects of ascertainment bias of both arrays were negligible for deciphering 33 global genetic trends of diversity in this panel and for estimating relatedness. We developed 34 an original approach based on linkage disequilibrium (LD) extent in order to determine 35 whether SNPs significantly associated with a trait and that are physically linked should be 36 considered as a single QTL or several independent QTLs. Using this approach, we showed 37 that the combination of the three technologies, which have different SNP distribution and 38 density, allowed us to detect more Quantitative Trait Loci (QTLs, gain in power) and 39 potentially refine the localization of the causal polymorphisms (gain in position).

40 **Conclusions:** Conceptually different technologies are complementary for detecting QTLs by 41 tagging different haplotypes in association studies. Considering LD, marker density and the 42 combination of different technologies (arrays and re-sequencing), the genotypic data presently 43 available were most likely enough to well represent polymorphisms in the centromeric 44 regions, whereas using more markers would be beneficial for telomeric regions.

45 Keywords: GWAS, linkage disequilibrium, genome coverage, maize, high-throughput
46 genotyping technologies.

2

47 Background

48 Understanding the genetic bases of complex traits involved in the adaptation to biotic and 49 abiotic stress in plants is a pressing concern, with world-wide drought due to climate change 50 as a major source of human food and agriculture threats. Recent progress in next generation 51 sequencing and genotyping array technologies contribute to a better understanding of the 52 genetic basis of quantitative trait variation by performing Genome-Wide Association Studies 53 (GWAS) on large diversity panels [1]. Single Nucleotide Polymorphism (SNP)-based 54 techniques became the most commonly used genotyping methods for GWAS because SNPs 55 are cheap, numerous, codominant and can be automatically analysed with SNP-arrays or 56 produced by genotyping-by-sequencing (GBS), or sequencing [2-4]. The decreasing cost of 57 genotyping technologies have led to an exponential increase in the number of markers used 58 for the GWAS in association panels, thereby raising the question of computation time to 59 perform the association tests. Computational issues were addressed by using either 60 approximate methods by avoiding re-estimating variance component for each SNP [5] or 61 exact methods using mathematical tools for sparing time in matrix inversion [6, 7]. It is 62 noteworthy that using approximate computation in GWAS can produce inaccurate p-values 63 when the SNP effect size is large or/and when the sample structure is strong [8].

Several causes may impact the power of Quantitative Trait Locus (QTL, locus involved in quantitative trait variation) detection in GWAS. Highly diverse panels have in general undergone multiple historical recombinations, leading to a low extent of linkage disequilibrium (LD). However, these panels can present different average and local patterns of LD [9-11]. A high marker density and a proper distribution of SNPs are therefore essential to capture causal polymorphisms. Furthermore, minor allele frequencies (MAF), population stratification and cryptic relatedness are three other important parameters affecting power and

false positive detection [12, 14]. These last two factors are substantial in several cultivated species such as maize [15] and grapevine [16], and their impact on LD can be statistically evaluated [17]. Population structure and kinship can be estimated using molecular markers [18-21] and can be modelled to efficiently detect marker-trait associations due to linkage only [12, 22, 23]. These advances have largely increased the power and effectiveness of linear mixed models that can now efficiently account for population structure and relatedness in GWAS [12, 8].

78

79 In maize, an Illumina Infinium HD 50,000 SNP-array (50K array) was developed by Ganal et 80 al. [3] and has been used extensively for diversity and association studies [24, 25]. For 81 example, GWAS were conducted to unravel the genetic architecture of phenology, yield 82 component traits and to identify several flowering time QTLs linked to adaptation of tropical 83 maize to temperate climate [26, 27]. With the same array, Rincent et al. [11] showed that LD 84 occurs over a longer distance in a dent than in a flint panel, with appreciable effects on the 85 power of QTL detection. Comparison of LD extent between association panels suggests that 86 genotyping with 50K markers causes a limited power of GWAS in many panels due to the 87 low LD extent and the correlation between allelic values at some SNPs due to the kinship and 88 population structure [14, 27]. Therefore, higher marker densities are desirable because the 89 maize genome size is large (2.4 Gb), the level of diversity is high, and LD extent is low (more 90 than one substitution per hundred nucleotides) [28]. As a consequence, an Affymetrix Axiom 91 600,000 SNP-array (600K array) was developed and used in association genetics [29, 30] and 92 detection of selective sweep [4]. Another possibility is whole genome sequencing, but this is 93 currently unpractical for large genomes such as maize because of the associated cost. Hence, a 94 Genotyping-By-Sequencing (GBS) procedure has been developed [2] that targets low-copy

95 genomic regions by using cheap restriction enzymes. Genotyping-by-sequencing has been 96 successfully used in maize for genomic prediction [31]. Romay *et al.* [32] and Gouesnard *et* 97 *al.* [33] highlighted the interest of the GBS for (i) deciphering and comparing the genetic 98 diversity of the inbred lines in seedbanks and (ii) identifying QTLs by GWAS for kernel 99 colour, sweet corn and flowering time. To our knowledge, the respective interests of DNA 100 arrays and GBS for diversity analyses and GWAS have never been compared in plants.

101

102 The main drawback of the DNA arrays is that they do not allow to discover new SNPs. This 103 possibly leads to some ascertainment bias in diversity analysis when the SNPs selected for 104 building arrays come from (i) the sequencing of a set of individuals who did not well 105 represent the diversity explored in the studied panel, (ii) a subset of SNPs that skews the 106 allelic frequency profile towards the intermediate frequencies [27, 34]. Ascertainment bias 107 can compromise the ability of the SNP arrays to reveal an exact view of the genetic diversity 108 [34]. Genotyping-by-sequencing can overcome ascertainment bias since it is based on 109 sequencing and therefore allows the discovery of alleles in the diversity panel analysed. It can 110 be generalized to any species at a low cost providing that numerous individuals have been 111 sequenced in order to build a representative library of short haplotypes to call SNPs [35]. 112 Non-repetitive regions of genomes can be targeted with two- to three-fold higher efficiency, 113 thereby considerably reducing the computationally challenging problems associated with 114 alignment in species with high repeat content. However, GBS may have a low-coverage 115 leading to a high missing data rate (65% in both studies; [32, 33]) and heterozygote under-116 calling, depending on genome size and structure, and on the number of samples combined in 117 the flow-cell. Furthermore, GBS requires the establishment of demanding bioinformatic 118 pipelines and imputation algorithms [36]. Pipelines have been developed to call SNP

genotypes from raw GBS sequence data and to impute the missing data from a haplotypelibrary [35, 36].

121 Here, we investigated the impact of using GBS and DNA arrays on the quality of the 122 genotyping data, together with the biological properties of data generated by these 123 technologies, and the potential complementarity of these approaches. In particular, we 124 analyzed the impact of increasing the marker density and using different genotyping 125 technologies (sequencing vs array) on (i) the estimates of relatedness and population structure, 126 (ii) the detection of QTLs (power. To address these issues, we performed a GWAS based on 127 genotypic datasets obtained using either GBS or DNA arrays with low (50k) or high (600k) 128 densities on a diversity panel of maize hybrids obtained from a cross of dent lines with a 129 common flint tester. Three traits were considered, namely grain yield, plant height and male 130 flowering time (day to anthesis), measured in 22 different environments (sites \times years \times 131 treatments) over Europe. We developed an original approach based on LD extent in order to 132 determine whether SNPs significantly associated with a trait should be considered as a single 133 QTL or several independent QTLs.

134

135 **Results**

Combining Tassel and Beagle imputations improved the genotyping quality for GBS

We estimated the genotyping and imputation concordance of the GBS based on common markers with the 50K or 600K arrays (Additional file 1: Figure S1 and Table S1). After SNP calling from reads using AllZeaGBSv2.7 database (direct reads, GBS₁, Additional file 1: Figure S1), the call rate was 33.81% on the common SNPs with the 50K array, *vs* 37% for the

140 whole GBS dataset. The genotyping concordance rate was 98.88% (Additional file 1: Table 141 S1). After imputation using *TASSEL* by Cornell Institute (GBS₂), the concordance rate was 142 96.04% on the common markers with the 50K array and 11.91% of missing data remained for 143 the whole GBS dataset. In GBS₃, all missing data were imputed by *Beagle* but yielded a lower 144 concordance rate (92.14% and 91.58% for the 50K and the 600K arrays). In an attempt to 145 increase the concordance rate of the genotyping while removing missing data, we tested two 146 additional methods, namely GBS₄ where the missing data and heterozygotes of Cornell 147 imputed data (GBS_2) were replaced by Beagle imputation, and GBS_5 where Cornell 148 homozygous genotypes (GBS₂) were completed by imputations from GBS₃ (Additional file 1: 149 Figure S1 and Table S1). GBS₅ displayed a slightly better concordance rate than GBS_2 150 (96.25% vs 96.04%) and predicted heterozygotes with a higher quality than GBS₄. GBS₅ was 151 therefore used for all genetic analyses and named GBS hereafter.

GBS displayed more rare alleles and lower call rate than microarrays

152 The SNP call rate was higher for the arrays (average values of 96% and >99% for the 50K 153 and 600K arrays, respectively), than for the GBS (37% for the direct reads). The MAF 154 distribution differed between the technologies (Figure 1): while the use of arrays resulted in a 155 near-uniform distribution, GBS resulted in an excess of rare alleles with a L-shaped 156 distribution (22% of SNPs with MAF < 0.05 for the GBS versus 6% and 9% for the 50K and 157 600K, respectively). This is not surprising since the 50K array was based on 27 sequenced 158 lines for SNPs discovery [3], the 600K array was based on 30 lines for [4], whereas GBS was 159 based on 31,978 lines, thereby leading to higher discovery of rare alleles. Consistent with 160 MAF distribution, the average gene diversity (He) was lower for GBS (0.27) than for arrays 161 (0.35 and 0.34 for the 50K and 600K arrays, respectively). The distribution of SNP

heterozygosity was similar for the three technologies, with a mean of 0.80%, 0.89% and 0.22 % for the 50K and 600K arrays and GBS, respectively. The heterozygosity of inbred lines was highly correlated between technologies with large coefficients of Spearman correlation: r_{50K} . $r_{500K} = 0.90$, r_{50K} -GBS = 0.76, r_{600K} -GBS = 0.83. The distribution of the SNPs along the genome was denser in the telomeres for the GBS and in the peri-centromeric regions for the 600K array, whereas the 50K array exhibited a more uniform distribution (top graph in Figure 2 and in Additional file 2: Figure S2).

Population structure and relatedness were consistent between the three technologies

169 We used the ADMIXTURE software to analyse the genetic structure within the studied panel 170 based on SNPs from the three technologies, by using two to ten groups. Based on a K-fold 171 cross-validation, the clustering in four genetic groups ($N_Q = 4$) was identified as the best one 172 in the datasets resulting from the three technologies. Considering a threshold of 0.5 (ancestral 173 fraction), the assignation to the four groups was identical except for a few admixed inbred 174 lines (Additional file 3: Figure S3). Based on the 50K, the four groups were constituted by (i) 175 39 lines in the Non Stiff Stalk (Iodent) family traced by PH207, (ii) 46 lines in the Lancaster 176 family traced by Mo17 and Oh43, and (iii) 55 lines in the stiff stalk families traced by B73 177 and (iv) 107 lines that did not fit into the three primary heterotic groups, such as W117 and 178 F7057. This organization appeared consistent with the organization of breeding programs into 179 heterotic groups, generally related to few key founder lines.

180

181 We compared two estimators of relatedness between inbred lines, IBS (Identity-By-State) and

182 K_Freq (Identity-By-Descend), calculated per technology. For IBS, pairs of individuals were

on average more related using the GBS data than those from arrays (Additional file 3: Table S2). Relatedness estimated with the two arrays were highly correlated: r = 0.95 and 0.98 for IBS and *K_Freq*, respectively (Figure 3 and Additional file 3: Figure S4b). The differences between the kinships estimated from the three technologies were reduced if the excess of rare alleles in the GBS was removed (Additional file 3: Figure S4c).

188

189 We further carried out diversity analyses by performing Principal Coordinate Analyses 190 (PCoA) on IBD (*K*_*Freq*, weights by allelic frequency) estimated from the three technologies. 191 The two first PCoA axes explained 12.9%, 15.6% and 16.3% of the variability for the GBS, 192 50K and 600K arrays, respectively. The same pattern was observed regardless of the 193 technology with the first axis separating the Stiff Stalk from the Iodent lines and the second 194 axis separating the Lancaster from the Stiff Stalk and Iodent lines (see illustration with the 195 50K kinship, Additionnal File 3: Figure S5). Key founders lines of the three heterotic groups 196 (Iodent: PH207, Stiff Stalk: B73, Lancaster: Mo17) were found at extreme positions along the 197 axes, which was consistent with the admixture groups previously described.

Long distance linkage disequilibrium was removed by taking into account population structure or relatedness

In order to evaluate the effect of kinship and the genetic structure on linkage disequilibrium (LD), we studied genome-wide LD between 29,257 PANZEA markers from the 50K array within and between chromosomes before and after taking into account the kinship (K_Freq estimated from the 50K array), structure (Number of groups = 4) or both (Additional file 4: Figure S6). Whereas inter-chromosomal LD was only partially removed when the genetic structure was taken into account, it was mostly removed when either the kinship or both

204 kinship and structure were considered (Additional file 4: Figure S6b and c). Accordingly, long 205 distance intra-chromosomal LD was almost totally removed for all chromosomes by 206 accounting for the kinship, structure or both. Interestingly, some pairs of loci located on 207 different chromosomes or very distant on a same chromosome remained in high LD despite 208 correction for genetic structure and kinship (Additional file 4: Figure S6). This can be 209 explained either by genome assembly errors, by chromosomal rearrangements such as 210 translocations or by strong epistatic interactions. Linkage disequilibrium decreased with 211 genetic or physical distance, Additional file 4: Figure S7). The majority of pairs of loci with 212 high LD ($r^2K > 0.4$) in spite of long physical distance (>30Mbp), were close genetically 213 (<3cM), notably on chromosome 3, 5, 7 and to a lesser extent 9 and 10. These loci were 214 located in centromeric and peri-centromeric regions that displayed low recombination rate, 215 suggesting that this pattern was due to variation of recombination rate along the chromosome. 216 Only very few pairs of loci in high LD were genetically distant (>5cM) but physically close 217 (<2Mbp). Linkage disequilibrium (r^2K and r^2KS) was negligible beyond 1 cM since 99% of 218 LD values were less than 0.12 in this case. Note that some unplaced SNPs remained in LD 219 after taking into account the kinship and structure with some SNPs with known positions on 220 chromosome 1, 3 and 4 (Additionnal File 4: Figure S6). Therefore, LD measurement 221 corrected by the kinship can help to map unplaced SNPs.

Linkage disequilibrium strongly differed between and within chromosomes

We combined the three technologies together to calculate the r^2K for all pairs of SNPs, which were genetically distant by less than 1 cM. For any chromosome region, LD extent in terms of genetic and physical distance showed a limited variation over the 100 sets of 500,000 loci pairs (cf. Material). This suggests that the estimation of LD extent did not strongly depend on

| 226 | our set of loci. LD extent varied significantly between chromosomes for both high |
|-----|--|
| 227 | recombinogenic (>0.5 cM/Mbp) and low recombinogenic regions (<0.5 cM/Mbp, Table 1). |
| 228 | Chromosome 1 had the highest LD extent in high recombination regions (0.062 \pm 0.007 cM) |
| 229 | and chromosome 9 the highest LD extent in low recombinogenic regions (898.6±21.7 kbp) |
| 230 | (Table 1). Linkage disequilibrium extent relative to genetic and physical distances was highly |
| 231 | and positively correlated in high recombinogenic regions ($r = 0.86$), whereas it was not in low |
| 232 | recombinogenic regions (r = -0.64). |
| | |

233

Table 1: Variation of LD extent, and percentage of genome covered.

| | | | | | | Chrom | osome | | | | | Whole | |
|-----------------------------|---------------|---------|---------|---------|---------|---------|---------|---------|---------|---------|---------|-----------|--|
| | | 1 | 2 | 3 | 4 | 5 | 6 | 7 | 8 | 9 | 10 | Genome | |
| Physical Size (| kbp) | 301,354 | 237,069 | 232,140 | 241,474 | 217,873 | 169,174 | 176,765 | 175,794 | 156,751 | 150,189 | 2,058,583 | |
| Genetic Size (cM) | | 268 | 211 | 188 | 150 | 205 | 129 | 148 | 182 | 145 | 139 | 1766 | |
| Physical LD extent (kbp) in | | | | | | | | | | | | | |
| Low Recombin | ation regions | 306 | 491 | 846 | 808 | 658 | 418 | 547 | 497 | 899 | 815 | 629 | |
| (<0.5 cM / Mb | p) | | | | | | | | | | | | |
| Genetic LD Extent (cM) in | | | | | | | | | | | | | |
| High Recombination | | 0.062 | 0.027 | 0.033 | 0.022 | 0.031 | 0.019 | 0.012 | 0.038 | 0.023 | 0.019 | 0.029 | |
| regions (>0.5 cM / Mbp) | | | | | | | | | | | | | |
| Percent of | 50K | 81% | 72% | 76% | 77% | 74% | 67% | 71% | 73% | 71% | 71% | 74% | |
| physical | 600K | 98% | 88% | 91% | 89% | 90% | 84% | 81% | 90% | 87% | 84% | 89% | |
| genome | GBS | 92% | 81% | 84% | 83% | 83% | 77% | 77% | 81% | 79% | 76% | 82% | |
| covered | Combined | 98% | 90% | 92% | 90% | 91% | 87% | 83% | 92% | 88% | 85% | 90% | |
| - | 50K | 72% | 41% | 44% | 38% | 41% | 32% | 24% | 46% | 32% | 27% | 42% | |
| Percent of | 600K | 96% | 71% | 76% | 68% | 72% | 62% | 47% | 78% | 63% | 53% | 71% | |
| genetic map covered | GBS | 86% | 58% | 61% | 53% | 61% | 48% | 37% | 63% | 48% | 40% | 58% | |
| covered | Combined | 97% | 74% | 78% | 72% | 74% | 65% | 51% | 81% | 66% | 57% | 74% | |

235 Genetic and Physical LD extent were obtained by adjusting Hill and Weir model's on

100 different sets of 500,000 loci randomly sampled in high and low recombination

237 regions, respectively. The value represented the average across these 100 sets. The

238 percentage of genome coverage was estimated using markers with MAF > 5% and

E(r^{2k}) = 0.1, for each technology and for the three technologies combined

240 (GBS+600K+50K).

241

The effective population size (*Ne*) estimated from the Hill and Weir's model [37] using genetic distance varied from 7.9 ± 0.04 (Chromosome 1) to 41.2 ± 0.12 (Chromosome 7) in high

244 recombinogenic regions. Noteworthy, the same approach lead to unrealistic values in low

recombinogenic regions (from 961 on Chromosome 6 to more than 1 million for chromosome
2 and 10), thereby confirming that the use of genetic distance is not well suited to model local
LD in low recombinogenic regions.

Finally, we studied the variation of local LD extent along each chromosome by adjusting the Hill and Weir's model against genetic distance within a sliding windows of 1cM (Additional file 4: Figure S8). After removing intervals that did not reach our criteria (Absence of model convergence, effective population size > 247, low number of loci), the 3,205 remaining intervals (90%) showed a high variation for genetic LD extent along each chromosome, with LD extent varying from 0.019 (Ne = 246) to 0.997 cM (Ne = 0.06) (Additional file 4: Figure S8).

Large differences in genome coverage between technologies

255 We estimated the percentage of the genome that was covered by LD windows around SNPs, 256 calculated by using either physical or genetic distances (Table 1). We observed a strong 257 difference in coverage between the three technologies at both genome-wide and chromosome 258 scale, as illustrated in Figure 2 on chromosome 3 (Table 1, and Additional file 2: Figure S2). 259 For a LD extent of $r^2K = 0.1$, 74%, 82% and 89% of the physical map, and 42%, 58% and 260 71% of the genetic map were covered by the 50K array, the GBS and the 600K array, 261 respectively (Table 1). For the combined data (50K + 600K + GBS), the coverage strongly 262 varied between chromosomes, ranging from 83% (chromosome 7) to 98% (chromosome 1) of 263 the physical map, and from 51% (chromosome 7) to 97% (chromosome 1) of the genetic map 264 (Table 1). For the physical map, increasing the LD extent threshold to $r^2K=0.4$ reduced the 265 genome coverage from 89% to 49% for 600K, 82% to 28% for GBS, 74% to 20% for 50K 266 and 90% to 52% for the combined data. Increasing the MAF threshold reduced slightly the

genome coverage, with smaller reduction for the physical map than genetic map. Surprisingly,
increasing the SNP number by combining the markers from the arrays and GBS did not
strongly increase the genome coverage as compared to the 600K, regardless of the threshold
for LD extent (Figure 2 and Additional file 2: Figure S2).
We observed a strong variation of genome coverage along each chromosome with contrasted
patterns in low and high recombinogenic regions (Figure 2 and Additional file 2: Figure S2).

While low recombinogenic regions were totally covered with all the technologies (except for few intervals using the 50K array), the genome coverage in high recombinogenic regions varied depending on both technology and SNP distribution. 47% of the 2Mbp intervals in high recombination regions were better covered by the 600K array than the GBS against only 1%, which were better covered by GBS than 600K.

278

Number of QTLs detected using genome-wide association studies increases with markers density

279 We observed a strong variation in the number of SNP significantly associated with the three 280 traits across the 22 environments (Table 2). The mean number of significant SNPs per 281 environment and trait was 3.7, 44.7, 17.9 and 62.4 for the 50K, 600K, GBS and the three 282 technologies combined, respectively (Table 3). Considering the p-value threshold used, 28, 283 303 and 204 false positives were expected among the 243, 2,953 and 1,182 associations 284 detected for 50K, 600K and GBS, respectively. False discovery rate appeared therefore higher 285 for GBS (17.2%) than for DNA arrays (11.5% and 10.2% for 50K and 600K, respectively). It 286 could be explained by the higher genotyping error rate of GBS due to imputation and/or by its 287 higher number of makers with a lower MAF. Both reduce the power of GBS compared to

288 DNA arrays and therefore lead to a higher false discovery rate. Proportionally to the SNP 289 number, 50K and 600K arrays resulted in 1.5- and 1.7-fold more associated SNPs per 290 situation (environment \times trait) than GBS (p-value<2x10⁻⁶, Table 3). This difference between 291 arrays and GBS was higher for grain yield (GY) and plant height (plantHT) than for male 292 flowering time (DTA, Table3). 293

- 294
- 295 **Table 2:** Number of significant SNPs per environment, per technology and for the

| | | Flo | wering 7 | Time | | | PI | ant Hei | ght | | Grain Yield | | | | |
|-------------|--------------|-----|----------|------|----------|--------------|-----|---------|------|----------|--------------|-----|------|------|----------|
| Environment | Heritability | 50K | 600K | GBS | Combined | Heritability | 50K | 600K | GBS | Combined | Heritability | 50K | 600K | GBS | Combined |
| Cam12R | 0.36 | 0 | 3 | 1 | 4 | 0.52 | 23 | 209 | 88 | 289 | 0.35 | 21 | 286 | 102 | 381 |
| Cam12W | 0.60 | 1 | 18 | 13 | 31 | 0.43 | 22 | 270 | 72 | 339 | 0.52 | 41 | 525 | 167 | 684 |
| Cam13R | 0.45 | 0 | 9 | 7 | 16 | 0.15 | 0 | 2 | 3 | 5 | 0.18 | 0 | 1 | 3 | 4 |
| Cra12R | 0.64 | 1 | 40 | 18 | 59 | 0.26 | 0 | 6 | 3 | 9 | 0.23 | 3 | 57 | 45 | 103 |
| Cra12W | 0.69 | 3 | 25 | 19 | 43 | 0.18 | 10 | 69 | 16 | 83 | 0.54 | 12 | 98 | 53 | 150 |
| Deb12R | 0.58 | 1 | 14 | 16 | 30 | 0.25 | 0 | 1 | 0 | 1 | 0.56 | 2 | 14 | 0 | 16 |
| Deb12W | 0.73 | 0 | 25 | 38 | 61 | 0.41 | 0 | 6 | 7 | 7 | 0.47 | 0 | 6 | 2 | 8 |
| Deb13R | 0.60 | 1 | 17 | 5 | 23 | 0.08 | 0 | 33 | 9 | 42 | 0.35 | 1 | 22 | 15 | 37 |
| Gai12R | 0.62 | 8 | 80 | 24 | 104 | 0.15 | 1 | 47 | 41 | 89 | 0.31 | 0 | 23 | 8 | 31 |
| Gai12W | 0.66 | 5 | 42 | 15 | 59 | 0.40 | 0 | 1 | 3 | 4 | 0.56 | 3 | 71 | 14 | 85 |
| Gai13R | 0.58 | 0 | 24 | 8 | 31 | 0.56 | 0 | 6 | 6 | 11 | 0.66 | 0 | 4 | 5 | 9 |
| Gai13W | 0.78 | 1 | 45 | 9 | 54 | 0.40 | 0 | 1 | 3 | 4 | 0.81 | 2 | 7 | 1 | 9 |
| Kar12R | 0.71 | 4 | 30 | 21 | 52 | 0.26 | 0 | 4 | 3 | 7 | 0.73 | 0 | 5 | 6 | 11 |
| Kar12W | 0.77 | 8 | 60 | 10 | 73 | 0.22 | 1 | 10 | 4 | 14 | 0.54 | 2 | 19 | 11 | 29 |
| Kar13R | 0.66 | 3 | 65 | 11 | 77 | 0.27 | 0 | 4 | 2 | 6 | 0.92 | 4 | 37 | 24 | 62 |
| Kar13W | 0.81 | 0 | 17 | 12 | 29 | 0.26 | 0 | 2 | 7 | 9 | 0.67 | 4 | 12 | 6 | 19 |
| Mur13R | 0.85 | 3 | 48 | 19 | 68 | 0.26 | 7 | 61 | 7 | 68 | 0.84 | 14 | 90 | 28 | 116 |
| Mur13W | 0.8 | 0 | 11 | 8 | 19 | 0.33 | 3 | 4 | 2 | 9 | 0.74 | 10 | 80 | 25 | 104 |
| Ner12R | 0.70 | 7 | 23 | 18 | 45 | 0.22 | 0 | 7 | 3 | 10 | 0.53 | 1 | 10 | 6 | 16 |
| Ner12W | 0.80 | 1 | 80 | 30 | 107 | 0.28 | 0 | 2 | 2 | 4 | 0.60 | 1 | 8 | 6 | 15 |
| Ner13R | 0.77 | 3 | 60 | 26 | 88 | 0.22 | 1 | 25 | 13 | 38 | 0.35 | 0 | 13 | 7 | 20 |
| Ner13W | 0.81 | 2 | 23 | 17 | 42 | 0.27 | 0 | 8 | 5 | 13 | 0.76 | 2 | 28 | 4 | 32 |
| Average | | 2.4 | 34.5 | 15.7 | 50.6 | | 3.1 | 35.4 | 13.6 | 48.4 | | 5.6 | 64.4 | 24.5 | 87.9 |
| Median | | 1 | 25 | 15.5 | 47.5 | | 0 | 6 | 4.5 | 9.5 | | 2 | 20.5 | 7.5 | 30 |

combined technologies.

The average, median and standard deviation (SD) per environment are calculated for each trait (male Flowering Time, Plant Height, Grain Yield).

299

300 Table 3: Comparison of associated SNPs and QTLs detected between traits and

301 three technologies.

| | - | | Signific | ant SNPs | | | Q | | |
|-------------|-----------|---------|----------|----------|----------|---------|---------|---------|----------|
| Technology | | 50K | 600K | GBS | Combined | 50K | 600K | GBS | Combined |
| Marker Nb | | 42046 | 459191 | 308929 | 810580 | 42046 | 459191 | 308929 | 810580 |
| | DTA | 52 | 759 | 345 | 1115 | 20 | 130 | 133 | 226 |
| Total Nb | plantHT | 68 | 778 | 299 | 1061 | 16 | 96 | 90 | 160 |
| Total ND | GY | 123 | 1416 | 538 | 1941 | 33 | 166 | 120 | 238 |
| | Per trait | 81 | 984 | 394 | 1372 | 23 | 131 | 114 | 208 |
| | DTA | 2.4 | 34.5 | 15.7 | 50.7 | 0.9 | 5.9 | 6.0 | 10.3 |
| Average per | plantHT | 3.1 | 35.4 | 13.6 | 48.2 | 0.7 | 4.4 | 4.1 | 7.3 |
| envir. | GY | 5.6 | 64.4 | 24.5 | 88.2 | 1.5 | 7.5 | 5.5 | 10.8 |
| | Per trait | 3.7 | 44.7 | 17.9 | 62.4 | 1.0 | 5.9 | 5.2 | 9.5 |
| | DTA | 5.70E-5 | 7.50E-5 | 5.10E-5 | 2.10E-5 | 2.20E-5 | 1.30E-5 | 2.00E-5 | 1.30E-5 |
| Average per | plantHT | 7.40E-5 | 7.70E-5 | 4.40E-5 | 2.00E-5 | 1.70E-5 | 9.50E-6 | 1.30E-5 | 9.00E-6 |
| SNP tested | GY | 1.30E-4 | 1.40E-4 | 7.90E-5 | 3.60E-5 | 3.60E-5 | 1.60E-5 | 1.80E-5 | 1.30E-5 |
| | Per trait | 8.80E-5 | 9.70E-5 | 5.80E-5 | 7.70E-5 | 2.50E-5 | 1.30E-5 | 1.70E-5 | 3.50E-5 |

302 QTLs were obtained by grouping associated SNPs with overlapping LD windows 303 (*LD_win*) for the three traits (DTA: male flowering time; PlantHT: plant height; GY: 304 grain yield). *Marker Nb*: is the number of markers tested in GWAS. *Total number*: is 305 the sum of associated SNPs or QTLs across environments. *Average per envir*.: is the 306 average number of QTLs obtained in 22 environments for three traits (66 trait-307 environments combinations). *Average per SNP tested*: is the number of associated 308 SNPs or QTLs detected divided by the number of SNP tested.

309

310

We used two approaches based on LD for grouping significant SNPs: (i) considering that all 311 312 SNPs with overlapping LD windows for $r^2K=0.1$ belong to the same QTL (LD_win) and (ii) 313 grouping significant SNPs that are adjacent on the physical map and are in LD ($r^2K > 0.5$, 314 LD_adj). The QTLs defined by using the two approaches were globally consistent since 315 significant SNPs within QTLs were in high LD whereas SNPs from different adjacent QTLs 316 were not (Additional file 6: Figure S9-LD-Adjacent and Additional file 7: Figure S9-LD-317 Windows). LD_adj detected more QTLs than LD_win for flowering time (242 vs 226), plant 318 height (240 vs 160) and grain yield (433 vs 237). The number of QTLs detected with the 319 LD adj approach increased strongly when the LD threshold was set above 0.5. Differences in 320 QTL groupings between the two methods were observed for specific LD and recombination 321 patterns. This occurred for instance on chromosome 6 for grain yield (Additional file 6:

322 Figure S9-LD-Adjacent and Additional file 7: Figure S9-LD-Windows). Within this region, 323 the recombination rate was low and the LD pattern between associated SNPs was complex. 324 While *LD_adj* splitted several SNPs in high LD into different QTLs (for instance QTL 232, 325 235, 237, 249), LD_win grouped together associated SNPs that are genetically close but 326 displayed a low LD (Additional file 6: Figure S9-LD-Adjacent and Additional file 7: Figure 327 S9-LD-Windows). Reciprocally, for flowering time, we observed different cases where 328 LD win separated distant SNPs in high LD into different QTLs whereas LD adj grouped 329 them (QTL 25 and 26, 51 to 53, 95 to 97, 208 and 209, 218 and 219). As these differences 330 were specific to complex LD and recombination patterns, we used the *LD_win* approach for 331 the rest of the analyses.

332

333 Although a large difference in number of associated SNPs was observed between 600K and 334 GBS, little difference was observed between QTL number after grouping SNPs (Table 2, 335 Table 3). The mean number of QTLs was indeed 1.0, 5.9 and 5.2 and 9.5 for the 50K, 600K, 336 GBS, and the three technologies combined, respectively (Table 3). Note that the number of 337 QTLs continued to increase with marker density when SNPs from GBS, 50K and 600K were 338 combined (Figure 4). The number of SNPs associated with each QTL varied according to the 339 technology (on average 3.7, 7.6, 3.4 and 6.6 significant SNPs for the 50K, 600K, GBS, and 340 the combined technologies, respectively). The total number of QTLs detected over all 341 environments by using the 600K array and GBS was close for flowering time (130 vs 133) 342 and plant height (96 vs 90). It was 1.4-fold higher for the 600K than GBS for grain yield (166 343 *vs* 120).

344

The 600K and GBS were highly complementary for association mapping

345 The 600K and GBS technologies were highly complementary to detect QTLs for the three 346 traits: 78%, 76% and 71% of the QTLs of flowering time, plant height and grain yield, 347 respectively, were specifically detected by 600K or GBS (Figure 5). On the contrary, 50K 348 displayed very few specific QTLs. While only 9 out 69 QTLs from the 50K array were not 349 detected when the 600K array was used, 39 QTLs detected using the 50K array were not 350 detected when using GBS. When we combined the GBS and 600K markers, 7% of their 351 common QTLs had $-log_{10}(Pval)$ increased by 2 and 21% by 1 potentially indicating a gain in 352 accuracy of the position of the causal polymorphism (Additional file 8: Table S3). 353 This complementarity between GBS and 600K is well exemplified with two strong 354 association peaks for flowering time on chromosome 1 (QTL32) and 3 (QTL95) detected in 355 several environments (Additional file 8: Table S3 and Figure 6a). In order to better understand 356 the origin of the complementarity between GBS and 600K technologies for GWAS, we 357 scrutinized the LD between SNPs and the haplotypes within these two QTLs (Figure 6b and c, 358 and Additional file 9: Figure S10 for other examples). For example, QTL95 showed a gain in

364 slightly above the significance threshold (Additional file 8: Table S3 and Figure 6b).

365

359

360

361

362

363

366 Haplotype analyses showed that the SNPs from the GBS within QTL95 were not able to 367 discriminate all haplotypes (Figure 6c). In QTL95, using the 600K markers allowed one to

power. It was only identified by the 600K array although the region included numerous SNPs

from GBS close to the associated peak. None of these SNPs was in high LD with the most

associated marker of the QTL95 (Figure 6b). Another example is QTL32, which was detected

by 1 to 10 GBS markers in 9 environments with -log(p-value) ranging from 5 to 7.6, whereas

it was detected by only two 600K markers in one environment (Ner12W) with -log(p-value)

368 discriminate the three main haplotypes (H1, H2, H3), whereas using the GBS markers did not 369 allow discrimination of H3 against H1 + H2. As H1 contributed to an earlier flowering time 370 than H2 or H3, associations appeared more significant for the 600K than for GBS (Figure 6c). 371 In QTL32, the use of GBS markers allowed identifying late individuals that mostly displayed 372 H1, H2 and H3 haplotypes, against early individuals that mostly displayed H4 and H5 373 haplotypes (Figure 6c). The gain of power for GBS markers as compared to 600K markers for 374 QTL32 originated from the ability to discriminate late individuals (black alleles) from early 375 individuals (red alleles) within H4 haplotypes (Figure 6c).

Stability, pleiotropy and distribution of QTL detected across environments

376 After combining the three technologies, we identified 226, 160, 238 QTLs for the flowering 377 time, plant height and grain yield, respectively (Table 3 and Additional file 8: Table S3). We 378 highlighted 23 QTLs with the strongest effects on flowering time, plant height and grain yield 379 $(-log_{10}(Pval) \ge 8, Table 4)$. The strongest association corresponded to the QTL95 for 380 flowering time $(-log_{10}(p-value) = 10.03)$ on chromosome 3 (158,943,646 - 159,005,990 bp), 381 the QTL135 for GY ($-log_{10}(p-value) = 18.7$) on chromosome 6 (12,258,527 - 29,438,316 bp) 382 and QTL78 on chromosome 6 (12,258,527 – 20,758,095 bp) for plant height ($-log_{10}(p-value)$) 383 = 17.31). The QTL95 for flowering time trait was the most stable QTLs across environments 384 since it was detected in 19 environments (Additional file 8: Table S3). Moreover, this QTL 385 showed a colocalization with OTL74 for grain yield in 5 environments and OTL30 for plant 386 height in 1 environment suggesting a pleiotropic effect. More globally, 472 QTLs appeared 387 trait-specific whereas 70 QTLs overlapped between at least two traits (6,3%, 5.2% and 3.0% 388 for GY and plantHT, GY and DTA, and DTA and plantHT, respectively) suggesting that 389 some QTLs are pleiotropic (Additional file 10: Figure S11). This is not surprising since

390 average corresponding correlations within environments for these traits were moderate (0.47,391 0.54 and 0.45, respectively). Only 0.7% overlapped between the three traits (Additional file 392 10: Figure S11). Twenty percent of QTLs were detected in at least two environments and 9% 393 in at least three environments (Additional file 10: Figure S12 and Table S4). We observed no 394 significant differences of stability between the three traits (p-value = 0.2). However, 6 out 7 395 most stable QTLs (Number of environments >5) were found for flowering time and a higher 396 proportion of QTLs were specific for plant height than grain yield and flowering time (85% vs 397 77% for both flowering time and grain yield, p-value = 0.09, p-value = 0.2), respectively. We 398 observed that QTLs that displayed a significant effect in more than one environment had 399 larger effects and -log(p-value) values than those significant in a single environment. This 400 difference in *-log(p-value)* values was stronger for grain yield and plant height than flowering 401 time.

402

403 **Table 4**: Summary of the main QTLs ($-log_{10}(Pval) \ge 8$) identified for the three traits.

| Trait | QTL | Chr | LowerLimit | UpperLimit | Pos | R2 | Effect | Log | MinorAll | MajorAll | MAF | EnvMax | NbDiffEnv |
|---------|-----|-----|------------|------------|-----------|------|--------|-------|----------|----------|------|--------|-----------|
| DTA | 95 | 3 | 158943646 | 159005990 | 158974594 | 0.15 | 1.27 | 10.03 | G | С | 0.41 | Ner13R | 19 |
| plantHT | 21 | 2 | 129971437 | 130912039 | 130441738 | 0.15 | -6.74 | 9.21 | Α | G | 0.14 | Cam12W | 3 |
| plantHT | 71 | 6 | 6593785 | 6636807 | 6614012 | 0.13 | -4.76 | 8.39 | G | A | 0.18 | Cam12R | 2 |
| plantHT | 72 | 6 | 6793841 | 6837747 | 6807230 | 0.14 | -4.87 | 8.77 | Т | G | 0.18 | Cam12R | 2 |
| plantHT | 78 | 6 | 12258527 | 20758095 | 20330595 | 0.27 | -8.99 | 17.31 | С | Т | 0.26 | Cam12W | 4 |
| plantHT | 79 | 6 | 21037721 | 23951687 | 22905376 | 0.19 | -5.45 | 11.42 | Т | G | 0.31 | Cam12R | 3 |
| plantHT | 80 | 6 | 24184017 | 26606537 | 25317825 | 0.13 | -4.41 | 8.17 | Т | С | 0.2 | Cam12R | 2 |
| plantHT | 81 | 6 | 26695327 | 28659766 | 28130108 | 0.16 | -5.14 | 9.84 | С | G | 0.44 | Cam12R | 2 |
| plantHT | 94 | 6 | 101463249 | 101501936 | 101482646 | 0.14 | -5.98 | 8.22 | Т | Α | 0.17 | Cam12W | 2 |
| plantHT | 110 | 8 | 12767198 | 12798330 | 12782777 | 0.19 | -7.67 | 12.44 | С | Т | 0.22 | Cam12W | 3 |
| GY | 65 | 3 | 140505559 | 144210207 | 141621777 | 0.12 | 0.42 | 8.13 | Α | С | 0.27 | Gai12W | 5 |
| GY | 85 | 3 | 186994852 | 187057772 | 187028970 | 0.12 | -0.48 | 8.49 | А | С | 0.28 | Kar12W | 1 |
| GY | 120 | 6 | 5131927 | 5177694 | 5155708 | 0.12 | -0.58 | 8.24 | С | Т | 0.42 | Cam12W | 2 |
| GY | 122 | 6 | 5623945 | 5659803 | 5638516 | 0.12 | -0.57 | 8.11 | Т | G | 0.23 | Cam12W | 2 |
| GY | 124 | 6 | 5855407 | 5887383 | 5871000 | 0.12 | -0.56 | 8.4 | Т | G | 0.42 | Cam12W | 2 |
| GY | 127 | 6 | 6593785 | 6636807 | 6612654 | 0.16 | -0.65 | 10.44 | С | А | 0.32 | Cam12W | 2 |
| GY | 128 | 6 | 6793841 | 6837747 | 6807462 | 0.12 | -0.54 | 8.41 | Α | С | 0.26 | Cam12W | 2 |
| GY | 129 | 6 | 6878877 | 6930838 | 6890199 | 0.12 | 0.63 | 8.06 | Т | А | 0.48 | Cam12W | 3 |
| GY | 130 | 6 | 7027497 | 7088575 | 7046773 | 0.13 | 0.62 | 8.71 | Α | G | 0.4 | Cam12W | 3 |
| GY | 131 | 6 | 7113662 | 7200479 | 7159714 | 0.12 | 0.59 | 8.24 | Т | С | 0.39 | Cam12W | 3 |
| GY | 135 | 6 | 12258527 | 29438316 | 18528943 | 0.28 | -0.78 | 18.7 | G | С | 0.31 | Cam12W | 6 |
| GY | 147 | 6 | 101463249 | 101501936 | 101482646 | 0.22 | -0.65 | 15.04 | Т | А | 0.17 | Cam12W | 5 |
| GY | 173 | 8 | 12767198 | 12798330 | 12782777 | 0.17 | -0.61 | 11.8 | С | Т | 0.22 | Cam12W | 4 |

404 "LowerLimit" and "UpperLimit" are the lower and upper physical limits for each QTL, 405 followed by the physical position (*Pos*, bp), proportion of the variance explained (R^2), 406 the effect of the major allele (*Effect*) as outputted by FastLMM, -log₁₀(**Pval**) (Log), the 407 minor and major alleles and the minor allele frequency (MAF) of the most significant 408 SNP within the QTL. The environment for which the most associated QTL was 409 observed (EnvMax) and the number of different environments (NbDiffEnv) that detected the QTL are shown. Note that QTLs 71-72 for the plant height and QTLs 410 411 129-130 for the grain yield are genetically close (<1cM) and display high mean LD 412 $(r^{2}K>0.5)$. Hence, QTLs 71-72 and 129-130 can potentially be merged.

413

The distribution of QTLs was not homogeneous along the genome since 82%, 77% and 79% of flowering time, plant height and grain yield QTLs, respectively, were located in the high recombinogenic regions, whereas they represented 46% of the physical genome (Additional file 10: Table S5 and Figure S13). The QTLs were more stable (≥ 2 environments) in low than in high recombinogenic regions (12.8% vs 5.8%, *p-value* = 0.03).

419 **Discussion**

GBS required massive imputation but displayed similar global trends than DNA arrays for genetic diversity organization

420 In order to reduce genotyping cost, GBS is most often performed at low depth leading to a 421 high proportion of missing data, thereby requiring imputation in order to perform GWAS. 422 Imputation can produce genotyping errors that can cause false associations and introduce bias 423 in diversity analysis [33]. We evaluated the quality of genotyping and imputation obtained by 424 different approaches, taking the 50K or 600K arrays as references. The best imputation 425 method that yielded a fully genotyped matrix with a low error rate for the prediction of both 426 heterozygotes and homozygotes was the approach merging the homozygous genotypes from 427 Tassel and the imputation of Beagle for the other data (GBS_5 in Additional file 1: Table S1). 428 The quality of imputation was high with 96% of allelic values consistent with those of the 429 50K and 600K arrays. This level of concordance is identical than in a study of USA national 430 maize inbred seed bank by Romay et al. [32]. It is higher than in a diversity study of 431 European flint maize collection (93%) by Gouesnard *et al.* [33], which was more distant from 432 the reference AllZeaGBSv2.7 database than for the panel presented here.

433

The ascertainment bias of arrays due to the limited number of lines used for SNP discovery was reinforced by counter-selection of rare alleles during the design process of DNA arrays [3, 4]. For GBS, the polymorphism database to call polymorphisms included thousands of diverse lines [35]. In our study, we used AllZeaGBSv2.7 database. After a first step of GBS imputation (GBS₂), missing data dropped to 11.9% *i.e.* only slightly more than in Romay *et al.* (10%) [34]. This confirms that the polymorphism database (AllZeaGBSv2.7) covered

440 adequately the genetic diversity of our genetic material.

441

Although, we observed differences of allelic frequency spectrum between GBS and DNA arrays, these technologies revealed similar trends in the organization of population structure and relatedness (Figure 1, Additional file 3: Figure S3 and S4 and Table S2) suggesting no strong ascertainment bias for deciphering global genetic structure trends in the panel. However, although highly correlated, level of relatedness differed between GBS and DNA arrays, especially when the lines were less related as showed by the deviation (to the left) of the linear regression from the bisector (Figure 3).

The extent of linkage disequilibrium strongly varied along and between chromosomes

449 Linkage disequilibrium extent in high recombinogenic regions varied to a large extent among 450 chromosomes, ranging from 0.012 to 0.062 cM. Similar variation of genetic LD extent 451 between maize chromosomes has been previously observed by Rincent et al. [14], but their 452 classification of chromosomes was different from ours. This difference could be explained by 453 the fact that we analyzed specifically high and low recombination regions. According to Hill 454 and Weir Model [37], the physical LD extent in a genomic region increased when the local 455 recombination rate decreased. As a consequence, chromosome 1 and 9 had the lowest and 456 highest physical LD extent and displayed the highest and one of the lowest recombination rate 457 in pericentromeric regions, respectively (0.26 vs 0.11 cM / Mbp), Table 1 and Additional file 458 10: Table S5). Unexpectedly, the genetic LD extent also correlated negatively with the 459 recombination rate. It suggested that chromosomes with a low recombination rate also display 460 a low effective population size. Background selection for deleterious alleles could explain this 461 pattern since it reduced the genetic diversity in low recombinogenic regions [38, 39]. Finally,

462 we observed a strong variation of the LD extent along each chromosome (Additional file 4: 463 Figure S8). As we used a consensus genetic map [40] that represents well the recombination 464 within our population, it suggested, according to Hill and Weir's model, that the number of 465 ancestors contributing to genetic diversity varied strongly along the chromosomes. This likely 466 reflects the selection of genomic regions for adaptation to environment or agronomic traits 467 [38], that leads to a differential contribution of ancestors according to their allelic effects. 468 Ancestors with strong favorable allele(s) in a genomic region may lead ultimately to large 469 identical by descent genomic segments [41].

SNPs were clustered into QTL highlighting interesting genomic regions

470 In previous GWAS, the closest associated SNPs were grouped into QTLs according to 471 either a fixed physical distance [1] or a fixed genetic distance [30, 42]. These approaches 472 suffer of two drawbacks. First, the physical LD extent can vary strongly along chromosomes 473 according to the variation of recombination rate (Additional file 2: Figure S2). Second, the 474 genetic LD extent depends both on panel composition and the position along the genome 475 (Table 1). These approaches may therefore strongly overestimate or underestimate the number 476 of QTLs. To address both issues Cormier et al. [43] proposed to group associated SNPs by 477 using a genetic window based on the genetic LD extent estimated by Hill and Weir model in 478 the genomic regions around the associated peaks [37]. In our study, we improved this last 479 approach (LD win):

480 - First, we used r^2K that corrected r^2 for kinship rather than the classical r^2 since r^2K 481 reflected the LD addressed in our GWAS mixed models to map QTL [17].

482 - Second, we took advantage of the availability of both physical and genetic maps of
483 maize to project the genetic LD extent on the physical map. This physical window was useful

484 to retrieve the annotation from B73 reference genome, decipher local haplotype diversity485 (Figure 6) and estimate physical genome coverage (Table 1, Figure 2).

Third, we considered an average LD extent estimated separately in the high and low
recombinogenic genomic regions. This average was estimated by using several large random
sets of pairs of loci in these regions rather than the local LD extent in the genomic regions
around each associated peaks.

490

We preferred this approach rather than using local LD extent in order to limit the effect of (i)
the strong variation of marker density along the chromosome (Additional file 2: Figure S2),
(ii) the local ascertainment bias due to the markers sampling (iii) the poor estimation of the
local recombination rate using a genetic map, notably for low recombination regions [3, 41]
(iv) errors in locus order due to assembly errors or chromosomal rearrangements.

496

497 We compared *LD_win* with *LD_adj*, another approach based on LD to group the SNPs 498 associated to trait variation into QTL. The discrepancies between the two approaches can be 499 explained by the local recombination rate and LD pattern. Since LD adj approach was based 500 on the grouping of contiguous SNPs according to their LD, this approach was highly sensitive 501 to (i) error in marker order or position due to genome assembly errors or structural variations, 502 which are important in maize [44] (ii) genotyping or imputation errors, which we estimated at 503 ca. 1% and ca. 4%, respectively, for GBS (Additional file 1: Table S1), (iii) presence of 504 allelic series with contrasted effects in different experiments which are currently observed in 505 maize [40], (iv) LD threshold used. On the other hand, LD_win lead either to inflate the 506 number of QTLs in high recombinogenic regions in which SNPs were too distant genetically 507 to be grouped, or deflated their number by grouping associated SNPs in low recombinogenic

regions. Since LD_win considered the average LD extent, this method could conduct either to separate or group abusively SNPs when local LD extent were different than the global LD extent.

511

512 Note that LD windows should not be considered as confidence intervals since the 513 relationship between LD and recombination is complex due to demography, drift and 514 selection in association panels, contrary to linkage based QTL mapping [17]. The magnitude 515 of the effect of causal polymorphism in the estimation of these intervals which is well 516 established for linkage mapping should be explored further [45]. Other approaches have been 517 proposed to cluster SNPs according to LD [46, 47]. These approaches aim at segmenting the 518 genome in different haplotype blocks separating by high recombination regions. These 519 methods are difficult to use for estimating putative windows inside which the causal 520 polymorphisms are because such approaches are not centered on the associated SNP.

521 Several QTLs identified by *LD_win* in our study correspond to regions previously 522 identified: in particular six regions associated with female flowering time [27] and 30 regions 523 associated with different traits in the Cornfed dent panel [11]. Conversely, we did not identify 524 in our study any QTL associated to the florigen ZCN8, which showed significant effect in 525 these two previous studies. This relates most likely to the fact that we narrowed the flowering 526 time range in our study, in particular by eliminating early lines. This reduced the 527 representation of the early allele in the Zcn8, leading to a MAF of 0.27 in our study vs. 0.35 in 528 Rincent et al. [11], which can diminishes the power of the tests [14].

Complementarity of 600K and GBS for QTL detection resulted mostly from the tagging of different haplotypes rather than the coverage of different genomic regions.

Number of significant SNPs and QTLs increased with the increase in marker number (Table 3, Figure 4). This could be explained partly by a better coverage of some genomic regions by SNPs, notably in high recombinogenic regions which showed a very short LD extent and were enriched in QTLs (Additional file 10: Figure S13). Numerous new QTLs identified by the 600K array and GBS as compared with those identified by the 50K array were detected in high recombinogenic regions that were considerably less covered by the 50K array than the 600K array or GBS (Additional file 2: Figure S2).

536

537 The high complementarity for QTL detection between GBS and 600K array was only 538 explained to a limited extent by the difference of the SNP distribution and density along the 539 genome, since these two technologies targeted similar regions as showed by coverage analysis 540 (Figure 2 and Additional file 2: Figure S2). However, at a finer scale, SNPs from the 600K 541 array and GBS could tag close but different genomic regions around genes. SNPs from the 542 600K array were mostly selected within coding regions of genes [4], whereas SNP from GBS 543 targeted more largely low copy regions, which included coding but also regulatory regions of 544 genes [32, 35]. To further analyse the complementarity of the technologies, we analysed local 545 haplotypes. We showed that both technologies captured different haplotypes when similar 546 genomic regions were targeted (Figure 6). Hence, we pinpointed that GBS and DNA arrays 547 are highly complementary for QTL detection because they tagged different haplotypes rather 548 than tagging different regions (Figure 6). Based on the L-shaped MAF distribution, which 549 suggest no ascertainment bias, and the high number of sequenced lines used for the GBS, we 550 expect a closer representation of the variation present in our panel by this technology

compared to the 600K array, but this comes to the cost of an enrichment in rare alleles. Both
factors tend to counterbalance each other in terms of GWAS power.

553

554 Our results suggest that we did not reach saturation with our c. 800,000 SNPs because (i) 555 some haplotypes certainly remain not tagged (ii) the genome coverage was not complete, and 556 (iii) the number of significant SNPs and QTLs continued to increase with marker density 557 (Figure 4). Considering LD and marker density, the genotypic data presently available were 558 most likely enough to well represent polymorphisms in the centromeric regions, whereas 559 using more markers would be beneficial for telomeric regions. New approaches based on 560 resequencing of representative lines and imputation are currently developed to achieve this 561 goal.

562

563 Methods

Plant Material and Phenotypic Data

564 The panel of 247 genotypes (Additional file 11: Table S6) includes 164 lines from a wider 565 panel of the CornFed project, composed of dent lines from Europe and America [11] and 83 566 additional lines derived from public breeding programs in Hungary, Italy and Spain and 567 recent lines free of patent from the USA. Lines were selected within a restricted window of 568 flowering time (10 days). Candidate lines with poor sample quality, i.e. high level of 569 heterozygosity, or high relatedness with other lines were discarded. The lines selection was 570 also guided by pedigree to avoid as far as possible over-representation of some parental 571 materials. These inbred lines were crossed with a common flint tester (UH007) and the

572 hybrids were evaluated for male flowering time (Day To Anthesis, DTA), plant height 573 (plantHT), and grain yield (GY) at seven sites in Europe, during two years (2012 and 2013), 574 and for two water treatments (watered and rainfed) [30]. The adjusted mean (Best Linear 575 Unbiased Estimation, BLUEs, <u>https://doi.org/10.15454/IASSTN</u>) of the three traits were 576 estimated per environment (site \times year \times treatment) using a mixed model with correction for 577 blocks, repetitions and rows and columns in order to take into account spatial variation of 578 micro-environment in each field trial [30]. Variance components and heritability of each traits 579 in each environment were also estimated [30] (Additional file 12: Table S7). Adjusted means 580 of hybrids were combined with genotyping data of the lines to perform GWAS.

Genotyping and Genotyping-By-Sequencing Data

581 The inbred lines were genotyped using three technologies: a maize Illumina Infinium HD 50K 582 array [3], a maize Affymetrix Axiom 600K array [4], and Genotyping-By-Sequencing [2, 35]. 583 In the arrays, DNA fragments are hybridized with probes attached to the array that flanked 584 SNPs that have been previously identified between inbred lines (Additional file 5: 585 Supplementary Text 1 for the description of the data from the two arrays). Genotyping-by-586 sequencing technology is based on multiplex resequencing of tagged DNA from different 587 individuals for which some genomic regions were targeted using restriction enzyme (Keygene 588 N.V. owns patents and patent applications protecting its Sequence Based Genotyping 589 technologies) [2]. Cornell Institute (NY, USA) processed raw sequence data using a multi-590 step Discovery and a one-top Production pipeline (TASSEL-GBS) in order to obtain genotypes 591 (Additional file 5: Supplementary Text 2). An imputation step of missing genotypes was 592 carried out by Cornell Institute [36], which utilized an algorithm that searches for the closest 593 neighbour in small SNP windows across the haplotype library [35], allowing for a 5%

594 mismatch. If the requirements were not met, the SNP was left ungenotyped for individuals.

595

596 We applied different filters (heterozygosity rate, missing data rate, minor allele frequency) for 597 a quality control of the genetic data before performing the diversity and association genetic 598 analyses. For GBS data, the filters were applied after imputation using the method 599 "Compilation of Cornell homozygous genotypes and Beagle genotypes" (GBS₅ in Additional 600 file 1: Figure S1; See section "Evaluating Genotyping and Imputation Quality"). We 601 eliminated markers that had an average heterozygosity and missing data rate higher than 0.15 602 and 0.20, respectively, and a Minor Allele Frequency (MAF) lower than 0.01 for the diversity 603 analyses and 0.05 for the GWAS. Individuals which had heterozygosity and/or missing data 604 rate higher than 0.06 and 0.10, respectively, were eliminated.

605

Evaluating Genotyping and Imputation Quality

606 Estimating the genotyping and imputation quality were performed using 245 lines since two 607 inbred lines have different seedlots between technologies. The 50K and the 600K arrays were 608 taken as reference to compare the concordance of genotyping (genotype matches) with the 609 imputation of GBS based on their position. While SNP position and orientation from GBS 610 were called on the reference maize genome B73 AGP_v2 (release 5a) [48], flanking 611 sequences of SNPs in the 50K array were primary aligned on the first maize genome reference 612 assembly B73 AGP_v1 (release 4a.53) [49]. Both position and orientation scaffold carrying 613 SNPs from the 50K array can be different in the AGP_v2, which could impair correct 614 comparison of genotype between the 50K array and GBS. Hence, we aligned flanking 615 sequences of SNPs from the 50K array on maize B73 AGP_v2 using the Basic Local

616 Alignment Search Tool (BLAST) to retrieve both positions and genotype in the same and 617 correct strand orientation (forward) to compare genotyping. The number of common markers 618 between the 50K/600K, 50K/GBS, GBS/600K and 50K/600K/GBS was 36,395, 7,018, 619 25,572 and 5,947 SNPs, respectively. The comparison of the genotyping and imputation 620 quality between the 50K/GBS, 50K/600K and 600K/GBS was done on 5,336 and 24,286 621 PANZEA markers [50] in common, and 26,154 markers in common, respectively. The 622 genotyping concordance of the 600K with the 50K array was extremely high (99.50%) but 623 slightly lower for heterozygotes (92.88%). In order to achieve these comparisons, we 624 considered the direct reads from GBS (GBS₁) and four approaches for imputation (GBS₂ to 625 GBS₅, Additional file 1: Figure S1). GBS₂ approach consisted in one imputation step from the 626 direct read by Cornell University, using TASSEL software, but missing data was still present. 627 **GBS**₃ approach consisted in a genotype imputation of the whole missing data of the direct 628 read by Beagle v3 [13]. In GBS₄, genotype imputation by Beagle was performed on Cornell 629 imputed data after replacing the heterozygous genotypes into missing data. GBS₅, consisted in 630 homozygous genotypes of GBS₂ completed by values imputed in GBS₃ (Additional file 1: 631 Figure S1).

Diversity Analyses

After excluding the unplaced SNPs and applying the filtering criteria for the diversity analyses (MAF > 0.01), we obtained the final genotyping data of the 247 lines with 44,729 SNPs from the 50K array, 506,662 SNPs from the 600K array, and 395,024 SNPs from the GBS (Figure 1). All markers of the 600K array and GBS₅ that passed the quality control were used to perform the diversity analyses (estimation of Q genetic groups and K kinships). For the 50K, we used only the PANZEA markers (29,257 SNPs) [50] in order to reduce the

ascertainment bias noted by Ganal *et al.* [3] when estimating Nei's index of diversity [51] and relationship coefficients. Genotypic data generated by the three technologies were organized as *G* matrices with *N* rows and *L* columns, *N* and *L* being the panel size and number of markers, respectively. Genotype of individual *i* at marker *l* ($G_{i,l}$) was coded as 0 (the homozygote for an arbitrarily chosen allele), 0.5 (heterozygote), or 1 (the other homozygote). Identity-By-Descend (IBD) was estimated according to Astle and Balding [19]:

644
$$K_Freq_{i,j} = \frac{1}{L} \sum_{l=1}^{L} \frac{(G_{i,l}-p_l)(G_{j,l}-p_l)}{p_l(1-p_l)},$$

645 where p_l is the frequency of the allele coded 1 of marker l in the panel of interest, i 646 and j indicate the inbred lines for which the kinship was estimated. We also estimated the 647 Identity-By-State (IBS) by estimating the proportion of shared alleles. For GWAS, we used 648 K_{Chr} [14] that are computed using similar formula as K_{Freq} , but with the genotyping data 649 of all the chromosomes except the chromosome of the SNP tested. This formula provides an 650 unbiased estimate of the kinship coefficient and weights by allelic frequency assuming Hardy-651 Weinberg equilibrium. Hence, relatedness is higher if two individuals share rare alleles than 652 common alleles.

653

Genetic structure was analysed using the sofware *ADMIXTURE v1.22* [18] with a number of groups varying from 2 to 10 for the three technologies. We compared assignation by *ADMIXTURE* of inbred lines between the three technologies by estimating the proportion of inbred lines consistently assigned between technologies two by two (50K *vs* GBS₅, 50K *vs* 600K, 600K *vs* GBS₅) using a threshold of 0.5 for admixture.

659

660 Expected heterozygosity (He) [51] was estimated at each marker as $2p_l(1 - p_l)$ and 661 was averaged on all the markers for a global characterization of the panel for the three

technologies. Principal Coordinate Analyses (PCoA) were performed on the genetic distance matrices [52], estimated as $I_{N,N} - K_Freq$, where $I_{N,N}$ is a matrix of ones of the same size as K_Freq .

Linkage Disequilibrium Analyses

We first analyzed the effect of the genetic structure and kinship on linkage disequilibrium (LD) extent within and between chromosomes by estimating genome-wide linkage disequilibrium using the 29,257 PANZEA SNPs from the 50K array. Four estimates of LD were used: the squared correlation (r^2) between allelic dose at two markers [53], the squared correlation taking into account global kinship with *K_Freq* estimator (r^2K), the squared correlation taking into account population structure (r^2S), and the squared correlation taking into account both (r^2KS) [17].

672

673 To explore the variation of LD decay and the stability of LD extent along the chromosomes, 674 we estimated LD between a non-redundant set of 810,580 loci from the GBS, the 50K and 675 600K arrays. To save computation time, we calculated LD between loci within a sliding 676 window of 1 cM. Genetic position was obtained by projecting the physical position of each 677 locus using a *smooth.spline* function R calibrated on the genetic consensus map of the Cornfed Dent Nested Association Mapping (NAM) design [40]. We used the estimator r^2 and 678 679 $r^{2}K$ using 10 different kinships K Chr. This last estimator was calculated because it 680 corresponds exactly to LD used to map QTL in our GWAS model. It determines the power of 681 GWAS to detect QTL considering that causal polymorphisms were in LD with some 682 polymorphisms genotyped in our panel [17]. To study LD extent variation, we estimated LD 683 extent by adjusting Hill and Weir's model [37] using non-linear regression (nls function in R-

684 package *nlme*) against both physical and genetic position within each chromosome. Since 685 recombination rate (cM / Mbp) varied strongly along the genome (Figure 2 and Additional 686 file 2: Figure S2), we defined high (>0.5 cM / Mbp) and low (<0.5 cM / Mbp) 687 recombinogenic genomic regions within each chromosome. We adjusted Hill and Weir's 688 model [37] separately in low and high recombinogenic regions (Additional file 10: Table S5) 689 by randomly sampling 100 sets of 500,000 pairs of loci distant from less than 1 cM. This 690 random sampling avoided over-representation of pairs of loci from low recombinogenic 691 regions due to the sliding-window approach (Additional file 12: Figure S14). 500,000 pairs of 692 loci represented 0.36% (Chromosome 3 / High rec) to 1.20% of all pairs of loci (Chromosome 693 8 / High rec).

For all analyses, we estimated LD extent by calculating the genetic and physical distance for the fitted curve of Hill and Weir's Model that reached $r^2K=0.1$, $r^2K=0.2$ and $r^2K=0.4$.

Genome coverage estimation

696 In order to estimate the genomic regions in which the effect of an underlying causal 697 polymorphisms could be captured by GWAS using LD with SNP from three technologies, we 698 developed an approach to define LD windows around each SNP with MAF \geq 5% based on 699 LD extent (Additional file 12: Figure S14). To set the LD window around each SNP, we used 700 LD extent with $r^2K=0.1$ (negligible LD), $r^2K=0.2$ (intermediate LD) and $r^2K=0.4$ (high LD) 701 estimated in low and high recombinogenic regions for each chromosome. We used the global 702 LD decay estimated for these large chromosomal regions rather than local LD extent (i) to 703 avoid bias due to SNP sampling within small genomic regions, (ii) to reduce computational 704 time, and (iii) to limit the impact of possible local error in genome assembly. In low 705 recombinogenic regions, we used the physical LD extent, hypothesizing that recombination

rate is constant along physical distance in these regions. In high recombinogenic regions, we used the genetic LD extent since there is a strong variation of recombination rate by base pair along the physical position (Additional file 2: Figure S2). We then converted genetic LD windows into physical windows by projecting the genetic positions on the physical map using the *smooth.spline* function implemented in R calibrated on the NAM dent consensus map [40]. Reciprocally, we obtained the genetic positions of LD windows in low recombinogenic regions by projecting the physical boundaries of LD windows on the genetic map.

713

To estimate coverage of the three technologies to detect QTLs based on their SNP distribution and density, we calculated cumulative genetic and physical length that are covered by LD windows around the markers, considering different LD extents for each chromosome $(r^2K=0.1, r^2K=0.2, r^2K=0.4)$. In order to explore variation of genome coverage along the chromosome, we estimated the proportion of genome covered using a sliding-windows approach based on physical distance (2Mbp).

Statistical Models for Association Mapping

720 We used four models to determine the statistical models that control best the confounding 721 factors (*i.e.* population structure and relatedness) in GWAS (Additional file 5: Supplementary 722 Texts 3 and 4). We tested different software implementing either approximate (EMMAX) [8] 723 or exact computation of standard test statistics (ASReml and FaST-LMM) [6, 54] for 724 computational time and GWAS results differences (Additional file 5: Supplementary Text 5). 725 Single-trait, single-environment GWAS was performed for each marker for each environment 726 and all traits using FaST-LMM. We selected the mixed model using K_Chr, estimated from 727 PANZEA markers of the 50K array to perform GWAS on 66 situations (environment \times trait)

(Additional file 5: Supplementary Text 4, Additional file 12: Figure S15 and Additional file 12: Figure S16). We developed a GWAS pipeline in R v3.2.1 [55] calling FaST-LMM software and implementing [14] approaches to conduct single trait and single environment association tests.

732

733 Multiple testing is a major challenge in GWAS using large numbers of markers. The 734 experiment-wise error rate (α_e) increases with the number of tests (number of markers) carried 735 out, even when the point-wise error rate (α_p) is maintained low. Popular methods [56, 57] are 736 overly conservative and can result in overlooking true positive associations. In addition, these 737 corrections assume that the hypothesis tests are independent. To take into account the 738 dependence of the tests in GWAS, α_p has to be adjusted in order to keep α_e at a nominal level. 739 Moskvina and Schmidt [58] and Gao et al. [59, 60] corrections can correctly infer the number 740 of independent tests and use the Bonferroni formula to rapidly adjust for multiple testing. 741 Using Gao approaches, we estimated the number of independent tests for GWAS at 15,780 742 for the 50K, 92,752 for the 600K, 109,117 for the GBS₅ and 191,026 for the combined genetic 743 data, leading to different *-log₁₀(p-value)* thresholds: 5.49, 6.27, 6.34 and 6.58, respectively. 744 Because of these differences, we used two thresholds of $-log_{10}(p-value) = 5$ (less stringent) 745 and 8 (hightly conservative and slightly above Bonferroni) for comparing GWAS to avoid the 746 differences of identification of significant SNPs between the technologies due to the choice of 747 the threshold.

748

Methods for grouping associated SNPs into QTLs

749 We used two approaches based on LD for grouping significant SNPs. The first approach 750 (LD win) used LD windows, previously described, to group significant SNPs into QTLs 751 considering that all SNPs with overlapping LD windows of $r^2K=0.1$ belong to the same QTL. 752 We hypothesized that significant SNPs with overlapping LD windows at $r^2K=0.1$ captured the 753 same causal polymorphism and were therefore a single and unique QTL. The second 754 approach (LD_adj) grouped into single QTL significant SNPs that are adjacent on the 755 physical map providing that their LD were above a LD threshold ($r^2K > 0.5$). We used LD 756 heatmaps for comparing the SNP grouping produced by the two approaches on the three 757 different traits across all environments (Additional file 6: Figure S9-LD-Adjacent and 758 Additional file 7: Figure S9-LD-Windows). All scripts are implemented in R software [55].

759 List of abreviations

- 760 DTA = Day to Anthesis
- 761 GY = Grain Yield adjusted at 15% moisture
- 762 plantHT = Plant Height
- 763 GBS = Genotyping By Sequencing
- 764 LD = Linkage disequilibrium
- 765 GWAS = Genome-Wide Association Studies
- 766 MAF = Minimum Allelic Frequency
- 767 SNP = Single Nucleotide Polymorphism
- 768 HRR = High Recombinogenic Regions
- 769 LRR = Low Recombinogenic Regions
- 770 QTL = Quantitative Trait Locus

771

772 **Declarations**

Ethics approval and consent to participate

773 Not applicable.

Consent for publication

774 Not applicable.

Availability of data and material

- The following links toward the data will be available upon publication of this paper.
- All the genotyping data used in this study can be found at <u>https://doi.org/10.15454/AEC4BN</u>.
- 777 The GWAS results can be found at <u>https://doi.org/10.15454/6TL2N4</u>.
- 778 The phenotypic dataset can be found at <u>https://doi.org/10.15454/IASSTN</u>.

Competing interests

The authors declare that they have no competing interests.

Funding

- 780 This project (Project ID: 244374) was funded under the European FP7- KBBE (CP IP -
- 781 Large-scale integrating project, DROPS) and the Agence Nationale de la Recherche project
- 782 ANR-10-BTBR-01 (ANR-PIA AMAIZING).

Authors' contributions

S.S.N., S.D.N. and A.C., designed the studied and wrote the article. S.S.N. performed genotyping data quality control, imputation and genetic analyses. S.D.N. developed and performed LD analyses. A.C. designed the association panel with the help of S.D.N. and C.W. C.B. participated in assembling the dent inbred lines panel, organizing the germplasms and field work for seeds production. E.J.M., C.W. and F.T. collected and analysed the phenotypic data. V.C. and D.M. performed DNA extraction and prepared the samples. All authors critically reviewed and approved the final manuscript.

Acknowledgements

790 We are grateful to key partners from the field: Pierre Dubreuil, Cécile Richard, Jérémy Lopez 791 (Biogemma), Tamás Spitkó (MTA ATK), Therese Welz (KWS), Franco Tanzi, Ferenc Racz, 792 Vincent Schlegel (Syngenta) and Maria Angela Canè (UNIBO). We also acknowledge Björn 793 Usadel and Axel Nagel (MPI) for data management. We thank Willem Kruijer, Fred Van 794 Eeuwijk (WUR), Tristan Mary-Huard and Laurence Moreau (INRA) for helpful discussions 795 and statistical advice. We are grateful to Chris-Carolin Schön (TUM) for providing an early 796 access to the Affymetrix Axiom 600K array and Edward Buckler (USDA) for providing 797 genotyping using GBS. We are also grateful to partners of the CornFed project, Univ. 798 Hohenheim (Germany), CSIC (Spain), CRAG (Spain), MTA ATK (Hungary), NCRPIS 799 (USA), CRB Maize (France) and CRA-MAC (Italy) who contributed to the genetic material.

Authors' information (optional)

800 Not applicable.

801 **References**

- 802
- 803

| 804 | 1. | Tian F, Bradbury PJ, Brown PJ, Hung H, Sun Q, | Flint-Garcia S. Rocheford TR. |
|-----|----|---|-------------------------------|
| | | | |

- 805 McMullen MD, Holland JB, Buckler ES: Genome-wide association study of leaf
- architecture in the maize nested association mapping population. *Nature Genetics*2011, 43:159.
- 808 2. Elshire RJ, Glaubitz JC, Sun Q, Poland JA, Kawamoto K, Buckler ES, Mitchell SE: A
- 809 Robust, Simple Genotyping-by-Sequencing (GBS) Approach for High Diversity
 810 Species. *PLoS ONE* 2011, 6: e19379.
- 811 3. Ganal MW, Durstewitz G, Polley A, Bérard A, Buckler ES, Charcosset A, Clarke JD,

812 Graner E-M, Hansen M, Joets J, et al: A Large Maize (Zea mays L.) SNP

- 813 Genotyping Array: Development and Germplasm Genotyping, and Genetic
- 814 Mapping to Compare with the B73 Reference Genome. *PLoS ONE* 2011, 6:
- 815 e28334.
- 816 4. Unterseer S, Bauer E, Haberer G, Seidel M, Knaak C, Ouzunova M, Meitinger T,
- 817 Strom TM, Fries R, Pausch H, et al: A powerful tool for genome analysis in maize:
- 818 development and evaluation of the high density 600 k SNP genotyping array.
- 819 *BMC Genomics* 2014, **15**:823.
- 820 5. Zhou X, Stephens M: Genome-wide efficient mixed-model analysis for association
 821 studies. *Nature Genetics* 2012, 44:821.
- 822 6. Lippert C, Listgarten J, Liu Y, Kadie CM, Davidson RI, Heckerman D: FaST linear
- 823 mixed models for genome-wide association studies. *Nature Methods* 2011, 8:833.
- 824 7. Listgarten J, Lippert C, Kadie CM, Davidson RI, Eskin E, Heckerman D: Improved

| 825 | | linear mixed models for genome-wide association studies. Nature Methods 2012, |
|-----|-----|--|
| 826 | | 9: 525. |
| 827 | 8. | Kang HM, Sul JH, Service SK, Zaitlen NA, Kong S-y, Freimer NB, Sabatti C, Eskin |
| 828 | | E: Variance component model to account for sample structure in genome-wide |
| 829 | | association studies. Nature Genetics 2010, 42:348. |
| 830 | 9. | Flint-Garcia SA, Thornsberry JM, Buckler ES: Structure of Linkage Disequilibrium |
| 831 | | in Plants. Annual Review of Plant Biology 2003, 54:357-374. |
| 832 | 10. | Remington DL, Thornsberry JM, Matsuoka Y, Wilson LM, Whitt SR, Doebley J, |
| 833 | | Kresovich S, Goodman MM, Buckler ES: Structure of linkage disequilibrium and |
| 834 | | phenotypic associations in the maize genome. Proceedings of the National Academy |
| 835 | | of Sciences 2001, 98: 11479. |
| 836 | 11. | Rincent R, Nicolas S, Bouchet S, Altmann T, Brunel D, Revilla P, Malvar RA, |
| 837 | | Moreno-Gonzalez J, Campo L, Melchinger AE, et al: Dent and Flint maize diversity |
| 838 | | panels reveal important genetic potential for increasing biomass production. |
| 839 | | Theoretical and Applied Genetics 2014, 127:2313-2331. |
| 840 | 12. | Yu J, Pressoir G, Briggs WH, Vroh Bi I, Yamasaki M, Doebley JF, McMullen MD, |
| 841 | | Gaut BS, Nielsen DM, Holland JB, et al: A unified mixed-model method for |
| 842 | | association mapping that accounts for multiple levels of relatedness. Nature |
| 843 | | Genetics 2006, 38: 203. |
| 844 | 13. | Browning SR, Browning BL. Rapid and Accurate Haplotype Phasing and Missing- |
| 845 | | Data Inference for Whole-Genome Association Studies By Use of Localized |
| 846 | | Haplotype Clustering. The American Journal of Human Genetics 2007, 81 (5): 1084- |
| 847 | | 1097 |
| 848 | 14. | Rincent R, Moreau L, Monod H, Kuhn E, Melchinger AE, Malvar RA, Moreno- |

| 849 | | Gonzalez J, Nicolas S, Madur D, Combes V, et al: Recovering Power in Association |
|-----|-----|--|
| 850 | | Mapping Panels with Variable Levels of Linkage Disequilibrium. Genetics 2014, |
| 851 | | 197: 375. |
| 852 | 15. | Van Inghelandt D, Melchinger AE, Lebreton C, Stich B: Population structure and |
| 853 | | genetic diversity in a commercial maize breeding program assessed with SSR and |
| 854 | | SNP markers. Theoretical and Applied Genetics 2010, 120:1289-1299. |
| 855 | 16. | Nicolas SD, Péros J-P, Lacombe T, Launay A, Le Paslier M-C, Bérard A, Mangin B, |
| 856 | | Valière S, Martins F, Le Cunff L, et al: Genetic diversity, linkage disequilibrium |
| 857 | | and power of a large grapevine (Vitis vinifera L) diversity panel newly designed |
| 858 | | for association studies. BMC Plant Biology 2016, 16:74. |
| 859 | 17. | Mangin B, Siberchicot A, Nicolas S, Doligez A, This P, Cierco-Ayrolles C: Novel |
| 860 | | measures of linkage disequilibrium that correct the bias due to population |
| 861 | | structure and relatedness. Heredity 2012, 108:285. |
| 862 | 18. | Alexander DH, Novembre J, Lange K: Fast model-based estimation of ancestry in |
| 863 | | unrelated individuals. Genome Research 2009, 19:1655-1664. |
| 864 | 19. | Astle W, Balding DJ: Population Structure and Cryptic Relatedness in Genetic |
| 865 | | Association Studies. Statist Sci 2009, 24:451-471. |
| 866 | 20. | Pritchard JK, Stephens M, Rosenberg NA, Donnelly P: Association Mapping in |
| 867 | | Structured Populations. The American Journal of Human Genetics 2000, 67:170- |
| 868 | | 181. |
| 869 | 21. | VanRaden PM: Efficient Methods to Compute Genomic Predictions. Journal of |
| 870 | | Dairy Science 2008, 91:4414-4423. |
| 871 | 22. | Bernardo R: Genomewide Markers for Controlling Background Variation in |
| 872 | | Association Mapping. The Plant Genome 2013, 6. |

| 873 | 23. | Thornsberry JM, Goodman MM, Doebley J, Kresovich S, Nielsen D, Buckler ES: |
|-----|-----|--|
| 874 | | Dwarf8 polymorphisms associate with variation in flowering time. Nature |
| 875 | | <i>Genetics</i> 2001, 28: 286. |
| 876 | 24. | Hufford MB, Lubinksy P, Pyhäjärvi T, Devengenzo MT, Ellstrand NC, Ross-Ibarra J: |
| 877 | | The Genomic Signature of Crop-Wild Introgression in Maize. PLOS Genetics |
| 878 | | 2013, 9: e1003477. |
| 879 | 25. | Rincent R, Laloë D, Nicolas S, Altmann T, Brunel D, Revilla P, Rodríguez VM, |
| 880 | | Moreno-Gonzalez J, Melchinger A, Bauer E, et al: Maximizing the Reliability of |
| 881 | | Genomic Selection by Optimizing the Calibration Set of Reference Individuals: |
| 882 | | Comparison of Methods in Two Diverse Groups of Maize Inbreds (Zea Mays L.). |
| 883 | | Genetics 2012, 192: 715. |
| 884 | 26. | Bouchet S, Bertin P, Presterl T, Jamin P, Coubriche D, Gouesnard B, Laborde J, |
| 885 | | Charcosset A: Association mapping for phenology and plant architecture in maize |
| 886 | | shows higher power for developmental traits compared with growth influenced |
| 887 | | traits. Heredity 2017, 118:249-259. |
| 888 | 27. | Bouchet S, Servin B, Bertin P, Madur D, Combes V, Dumas F, Brunel D, Laborde J, |
| 889 | | Charcosset A, Nicolas S: Adaptation of Maize to Temperate Climates: Mid- |
| 890 | | Density Genome-Wide Association Genetics and Diversity Patterns Reveal Key |
| 891 | | Genomic Regions, with a Major Contribution of the Vgt2 (ZCN8) Locus. PLoS |
| 892 | | ONE 2013, 8:e71377. |
| 893 | 28. | Messing J, Dooner HK: Organization and variability of the maize genome. Current |
| 894 | | Opinion in Plant Biology 2006, 9:157-163. |
| 895 | 29. | Hu H, Schrag TA, Peis R, Unterseer S, Schipprack W, Chen S, Lai J, Yan J, Prasanna |
| 896 | | BM, Nair SK, et al: The Genetic Basis of Haploid Induction in Maize Identified |

| 897 | | with a Novel Genome-Wide Association Method. Genetics 2016, 202:1267. |
|-----|-----|---|
| 898 | 30. | Millet EJ, Welcker C, Kruijer W, Negro S, Coupel-Ledru A, Nicolas SD, Laborde J, |
| 899 | | Bauland C, Praud S, Ranc N, et al: Genome-Wide Analysis of Yield in Europe: |
| 900 | | Allelic Effects Vary with Drought and Heat Scenarios. Plant Physiology 2016, |
| 901 | | 172: 749. |
| 902 | 31. | Crossa J, Beyene Y, Kassa S, Pérez P, Hickey JM, Chen C, de los Campos G, |
| 903 | | Burgueño J, Windhausen VS, Buckler E, et al: Genomic Prediction in Maize |
| 904 | | Breeding Populations with Genotyping-by-Sequencing. G3: |
| 905 | | Genes/Genetics 2013, 3:1903. |
| 906 | 32. | Romay MC, Millard MJ, Glaubitz JC, Peiffer JA, Swarts KL, Casstevens TM, Elshire |
| 907 | | RJ, Acharya CB, Mitchell SE, Flint-Garcia SA, et al: Comprehensive genotyping of |
| 908 | | the USA national maize inbred seed bank. Genome Biology 2013, 14:R55. |
| 909 | 33. | Gouesnard B, Negro S, Laffray A, Glaubitz J, Melchinger A, Revilla P, Moreno- |
| 910 | | Gonzalez J, Madur D, Combes V, Tollon-Cordet C, et al: Genotyping-by-sequencing |
| 911 | | highlights original diversity patterns within a European collection of 1191 maize |
| 912 | | flint lines, as compared to the maize USDA genebank. Theoretical and Applied |
| 913 | | Genetics 2017, 130:2165-2189. |
| 914 | 34. | Frascaroli E, Schrag TA, Melchinger AE: Genetic diversity analysis of elite |
| 915 | | European maize (Zea mays L.) inbred lines using AFLP, SSR, and SNP markers |
| 916 | | reveals ascertainment bias for a subset of SNPs. Theoretical and Applied Genetics |
| 917 | | 2013, 126: 133-141. |
| 918 | 35. | Glaubitz JC, Casstevens TM, Lu F, Harriman J, Elshire RJ, Sun Q, Buckler ES: |
| 919 | | TASSEL-GBS: A High Capacity Genotyping by Sequencing Analysis Pipeline. |
| 920 | | <i>PLoS ONE</i> 2014, 9: e90346. |

| 36. | Swarts K, Li H, Romero Navarro JA, An D, Romay MC, Hearne S, Acharya C, |
|-----|--|
| | Glaubitz JC, Mitchell S, Elshire RJ, et al: Novel Methods to Optimize Genotypic |
| | Imputation for Low-Coverage, Next-Generation Sequence Data in Crop Plants. |
| | The Plant Genome 2014, 7. |
| 37. | Hill WG, Weir BS: Variances and covariances of squared linkage disequilibria in |
| | finite populations. Theoretical Population Biology 1988, 33:54-78. |
| 38. | Charlesworth D, Willis JH: The genetics of inbreeding depression. Nature Reviews |
| | Genetics 2009, 10:783. |
| 39. | Hudson RR, Kaplan NL: Deleterious background selection with recombination. |
| | Genetics 1995, 141:1605. |
| 40. | Giraud H, Bauland C, Falque M, Madur D, Combes V, Jamin P, Monteil C, Laborde J, |
| | Palaffre C, Gaillard A, et al: Reciprocal Genetics: Identifying QTL for General |
| | and Specific Combining Abilities in Hybrids Between Multiparental Populations |
| | from Two Maize (Zea mays L.) Heterotic Groups. Genetics 2017, 207:1167. |
| 41. | Bauer E, Falque M, Walter H, Bauland C, Camisan C, Campo L, Meyer N, Ranc N, |
| | Rincent R, Schipprack W, et al: Intraspecific variation of recombination rate in |
| | maize. Genome Biology 2013, 14:R103. |
| | |
| | |
| | |
| | |
| 41. | Tian F, Bradbury PJ, Brown PJ, Hung H, Sun Q, Flint-Garcia S, Rocheford TR, |
| | McMullen MD, Holland JB, Buckler ES: Genome-wide association study of leaf |
| | architecture in the maize nested association mapping population. Nature Genetics |
| | 37. 38. 39. 40. |

| 945 | | 2011, 43: 159. |
|-----|-----|---|
| 946 | 42. | Le Gouis J, Bordes J, Ravel C, Heumez E, Faure S, Praud S, Galic N, Remoué C, |
| 947 | | Balfourier F, Allard V, Rousset M: Genome-wide association analysis to identify |
| 948 | | chromosomal regions determining components of earliness in wheat. Theoretical |
| 949 | | and Applied Genetics 2012, 124: 597-611. |
| 950 | 43. | Cormier F, Le Gouis J, Dubreuil P, Lafarge S, Praud S: A genome-wide |
| 951 | | identification of chromosomal regions determining nitrogen use efficiency |
| 952 | | components in wheat (Triticum aestivum L.). Theoretical and Applied Genetics |
| 953 | | 2014, 127: 2679-2693. |
| 954 | 44. | Springer NM, Ying K, Fu Y, Ji T, Yeh C-T, Jia Y, Wu W, Richmond T, Kitzman J, |
| 955 | | Rosenbaum H, et al: Maize Inbreds Exhibit High Levels of Copy Number |
| 956 | | Variation (CNV) and Presence/Absence Variation (PAV) in Genome Content. |
| 957 | | PLOS Genetics 2009, 5:e1000734. |
| 958 | 45. | Darvasi A, Weinreb A, Minke V, Weller JI, Soller M: Detecting marker-QTL |
| 959 | | linkage and estimating QTL gene effect and map location using a saturated |
| 960 | | genetic map. Genetics 1993, 134:943. |
| 961 | 46. | Gabriel SB, Schaffner SF, Nguyen H, Moore JM, Roy J, Blumenstiel B, Higgins J, |
| 962 | | DeFelice M, Lochner A, Faggart M, et al: The Structure of Haplotype Blocks in the |
| 963 | | Human Genome. Science 2002, 296:2225. |
| 964 | 47. | Wang H, Chu WS, Hemphill C, Elbein SC: Human Resistin Gene: Molecular |
| 965 | | Scanning and Evaluation of Association with Insulin Sensitivity and Type 2 |
| 966 | | Diabetes in Caucasians. The Journal of Clinical Endocrinology & Metabolism 2002, |
| 967 | | 87: 2520-2524. |
| 968 | 48. | Schnable PS, Ware D, Fulton RS, Stein JC, Wei F, Pasternak S, Liang C, Zhang J, |

- 969 Fulton L, Graves TA, et al: **The B73 Maize Genome: Complexity, Diversity, and**
- 970 **Dynamics.** *Science* 2009, **326:**1112.
- 971 49. Ganal MW, Altmann T, Röder MS: SNP identification in crop plants. *Current*972 *Opinion in Plant Biology* 2009, 12:211-217.
- 973 50. Gore MA, Chia J-M, Elshire RJ, Sun Q, Ersoz ES, Hurwitz BL, Peiffer JA, McMullen
- 974 MD, Grills GS, Ross-Ibarra J, et al: A First-Generation Haplotype Map of Maize.
- 975 *Science* 2009, **326:**1115.
- 976 51. Nei M: Estimation of Average Heterozygosity and Genetic Distance from a Small
 977 Number of Individuals. *Genetics* 1978, 89:583.
- 978 52. Gower JC: Some distance properties of latent root and vector methods used in
- 979 **multivariate analysis.** *Biometrika* 1966, **53:**325-338.
- 980 53. Hill WG, Robertson A: Linkage disequilibrium in finite populations. *Theoretical*981 and Applied Genetics 1968, 38:226-231.
- 982 54. Butler DG, Cullis BR, Gilmour AR, Gogel BJ: ASReml-R reference manual. The
- 983 State of Queensland, Department of Primary Industries and Fisheries, Brisbane,
- 984 *Australia* 2009.
- 985 55. R Core Team: R: A language and environment for statistical computing. R
- 986 Foundation for Statistical Computing, Vienna, Austria 2015:URL https://www.R-
- 987 project.org/.
- 988 56. Bonferroni CE: Teoria statistica delle classi e calcolo delle probabilità.
- 989 Pubblicazioni dell'Istituto Superiore di Scienze Economiche e Commerciali di Firenze
 990 1936, 8:3-62.
- 991 57. Šidák Z: Rectangular Confidence Regions for the Means of Multivariate Normal
 992 Distributions. *Journal of the American Statistical Association* 1967, 62:626-633.

| 993 | 58. | Moskvina V, Schmidt KM: On multiple-testing correction in genome-wide |
|------|-----|---|
| 994 | | association studies. Genetic Epidemiology 2008, 32:567-573. |
| 995 | 59. | Gao X, Becker LC, Becker DM, Starmer JD, Province MA: Avoiding the high |
| 996 | | Bonferroni penalty in genome-wide association studies. Genetic Epidemiology |
| 997 | | 2010, 34: 100-105. |
| 998 | 60. | Gao X, Starmer J, Martin ER: A multiple testing correction method for genetic |
| 999 | | association studies using correlated single nucleotide polymorphisms. Genetic |
| 1000 | | <i>Epidemiology</i> 2008, 32: 361-369. |
| 1001 | | |
| 1002 | | |

1003 **Figure legends**

Figure 1: Comparison of genotyping data between 50K and 600K arrays, and GBS. (a) Distribution of minor allele frequency per SNP before filtering (monomorphic SNPs removed). (b) Distribution of SNP missing data proportion for the 50K array, 600K array, GBS direct reads (GBS₁) and GBS after imputation by Cornell Institute (GBS₂, note that the scale of the x-axes is different). (c) Relatedness distribution (Identity-By-State, IBS) after QC filtering with MAF≥1% (IBS using GBS₁ was not estimated because of the low calling rate).

1011 **Figure 2:** Variation of the markers density (top), the recombination rate (middle) and the 1012 genome coverage (bottom). Non-overlapping 2Mbp windows along the chromosome 3 were 1013 used. The percentage of genome coverage used the cumulative length of LD windows 1014 calculated around each SNP. Markers along chromosome 3 have MAF \geq 5%. Green, blue, red 1015 and black lines represent variation of GBS, 600K, 50K and combined technologies,

1017

1018 **Figure 3:** Correlation (*r*) of the Identity-By-State (IBS) between the three technologies (after 1019 imputation). (**a**) IBS_{600K} vs IBS_{50K}, (**b**) IBS_{GBS} vs IBS_{50K}, (**c**) IBS_{GBS} vs IBS_{600K}. The red line 1020 indicates the bisector.

1021

Figure 4: Number of significant SNPs (blue line) and QTLs (red line) identified as a function
of SNP density (x-axis) for the three traits (DTA, male flowering time; plantHT, plant height;
GY, grain yield).

Figure 5: Complementarity of the three technologies to detect QTLs. The numbers of specific
QTLs detected by each technologies for the three traits (flowering time, plant height, grain
yield) are shown.

1028 Figure 6: Complementarity of QTLs detection between the 600K array and the GBS for two 1029 regions (QTL 32/QTL95). (a) Manhattan plot of the $-log_{10}(p-value)$ along the genome. Dotted 1030 red lines correspond to QTL32 and QTL95 located on chromosome 1 and 3, respectively, for the flowering time in one environment (Ner13R). (b) Local manhattan plot of the $-log_{10}(p-1)$ 1031 *value*) (top) and linkage disequilibrium corrected by the kinship (r^2K) (bottom) of all SNPs 1032 1033 with the strongest associated marker within QTL 32 (left) and QTL 95 (right). (c) Local 1034 haplotypes displayed by SNPs within the QTLs 32 (left) and 95 (right). Inbred lines are in 1035 rows and SNPs are in columns. Inbred lines were ordered by hierarchical clustering based on 1036 local dissimilarity estimated by all SNPs within each QTLs. Genotyping matrix is colored 1037 according to their allelic dose at each SNP. Red and black represent homozygotes and gray 1038 represent heterozygotes. The associated peaks (red vertical lines) and other associated SNPs 1039 with $-log_{10}(p-value) > 5$ (orange vertical lines) are indicated above the genotyping matrix. H1,

1040 H2, H3, H4, H5 represent the 5 and 3 haplotypes obtained by cutting the dendograms with the 1041 most 5 and 3 dissimilar clusters within QTL32 and QTL95, respectively.

1042

1045

Additional file legends 1043

1044 Additional file 1 (.docx):

Figure S1: Different approaches used to compare the quality of genotyping and imputation of 1046 the GBS. We considered the direct reads from GBS (GBS_1) and four approaches for 1047 imputation (GBS₂ to GBS₅). GBS₂ approach consisted in one imputation step from the direct 1048 read by Cornell University, using TASSEL software, but missing data was still present. GBS₃ 1049 approach consisted in a genotype imputation of the whole missing data of the direct read by 1050 *Beagle v3.* In **GBS**₄, genotype imputation by Beagle was performed on Cornell imputed data 1051 after replacing the heterozygous genotypes into missing data. **GBS**₅, consisted in homozygous

1052 genotypes of GBS₂ completed by values imputed in GBS₃.

1053 Table S1: Percentage of GBS concordance based on the 50K and 600K arrays (Reference).

1054 Call rate of SNPs from GBS are in brackets. * After Beagle inference of missing data, the call

1055 rate is 100%. Here the call rate is <100% because the comparison was made against the 50K

1056 and the 600K arrays that include few missing data.

1057

1058 Additional file 2 (.pdf):

1059 Figure S2: Variation of the markers density, the recombination rate and the genome coverage 1060 in non-overlapping 2 Mbp windows along each chromosome. The percentage SNP coverage 1061 (bottom) used the cumulated length of physical LD windows around each SNP. Markers have 1062 MAF \geq 5%. Green, blue, red and black lines represent variation of GBS, 600K, 50K and

1063 combined technologies, respectively.

1064

- 1065 Additional file 3 (.docx):
- 1066 Figure S3: Contribution of four ancestral populations to 247 inbred lines after ADMIXTURE
- 1067 analysis. Markers from the 50K array (top), 600K array (middle) and GBS (bottom) were

1068 used. One vertical bar corresponds to one individual. Lines were ordered according to

1069 contributions observed for the 50K array. From left to right, we have Stiff Stalk lines type

- 1070 B73 and B14a (red), Iodent lines type PH207 (green), Lancaster lines type Mo17 and Oh43
- 1071 (turquoise), a group of lines assembling W117, F7057 type lines (blue).

1072 Table S2: Means and ranges of the two relatedness estimators (IBS and IBD *i.e.* K_Freq)

1073 from the 50K (29,257 PANZEA SNPs only) and 600K arrays, and GBS.

1074 Figure S4: Correlation (r) between the IBS and IBD (K_Freq) for each technology (A) and

1075 correlation of IBD between the three technologies (B). (C) Correlation of IBD between the

1076 three technologies after removing the excess of rare alleles in the GBS to have the same

1077 distribution of MAF as in the 50K and the 600K arrays. The red line is the bisector.

1078 Figure S5: Principal coordinate analyses (PCoA) of the DROPS panel. The PCoA were based

1079 on the covariance matrix K_Freq estimated from the 50K Illumina array. The genetic groups

1080 identified by ADMIXTURE ($N_Q = 4$) are colored (differently than in Fig. S6). Three key

1081 founders are indicated (Iodent: PH207 in red, Stiff Stalk: B73 in blueviolet, Lancaster: Mo17

1082 in turquoise).

1083

1084 Additional file 4 (.docx):

Figure S6: Heatmap of genome-wide linkage disequilibrium (LD) between all markers within
and between chromosomes using PANZEA SNPs from the 50K array. All SNPs were ordered

1087 according to their position on the genome. Dots represented LD between two loci and were 1088 colored according to their strength. Classical LD measurement r^2 between loci were 1089 represented within triangle below the diagonal. Linkage disequilibrium corrected for structure 1090 (r^2S , A), relatedness (r^2K , B) or both (r^2KS , C) were represented within triangle above the 1091 diagonal.

- 1092 **Figure S7:** Linkage disequilibrium (r^2 , top) and LD corrected for relatedness (r^2k , bottom) as
- 1093 a function of physical distance (left) and genetic distance (right): example of chromosome 1.
- 1094 Figure S8: Variation of genetic LD extent (Dm, cM), effective population size (N), along the
- 1095 physical map. A sliding window of 1 cM moving by 0.5 cM at each step was used. Local
- 1096 genetic LD extent (cM) and local effective size (N) were estimated by adjusting the Hill and
- 1097 Weir model's using r^2K between all loci that are located in sliding windows of 1 cM. Each
- 1098 values were plotted on the physical map of each chromosome by projecting the genetic
- 1099 position of the windows on the physical map.
- 1100
- 1101 Additional file 5 (.docx):
- 1102 **Supplementary Text 1:** Differences between microarrays.
- 1103 Supplementary Text 2: GBS pipelines.
- 1104 **Supplementary Text 3:** Statistical models for GWAS.
- 1105 **Supplementary Text 4:** Effects of confounding factors on GWAS.
- 1106 **Supplementary Text 5:** Performance of different software.
- 1107
- 1108 Additional file 6 (.pdf):
- 1109 Figure S9-LD_Windows: QTL limits obtained by the LD_win approach projected on
- 1110 heatmaps representing the level of LD between associated SNPs for each trait (DTA: male

1111 flowering time, plantHT: plant height and GY: grain yield) and each chromosome. Upper and 1112 lower triangles on the heatmaps represented the r^2 and r^2K values between associated SNPs, 1113 respectively. Linkage disequilibrium between loci was colored according to values from weak 1114 LD (yellow) to high LD (red). The significant markers were ordered according to their 1115 physical positions on the chromosome and were represented by ticks on the four sides of the 1116 heatmaps. Limits of QTLs were displayed by gray dotted lines. QTL numbers were indicated 1117 in gray on the top and the right of each heatmap.

1118

1119 Additional file 7 (.pdf):

1120 Figure S9-LD_Adjacent: QTL limits obtained by the LD_Adj approach projected on 1121 heatmaps representing the level of LD between associated SNPs for each trait (DTA: male 1122 flowering time, plantHT: plant height and GY: grain yield) for each chromosome. Upper and lower triangles on the heatmaps represented the r^2 and r^2K values between associated SNPs, 1123 1124 respectively. Linkage disequilibrium between loci was colored according to values from weak 1125 LD (yellow) to high LD (red). The significant markers were ordered according to their 1126 physical positions on the chromosome and were represented by ticks on the four sides of the 1127 heatmaps. Limits of QTLs were displayed by gray dotted lines. QTL numbers were indicated 1128 in gray on the top and the right of each heatmap.

1129

1130 Additional file 8 (.pdf):

Table S3: Summary of all the QTLs identified for the male flowering time (DTA), plant height (plantHT) and grain yield (GY). "LowerLimit" and "UpperLimit" columns are the lower and upper physical limits for each QTL. The "Rec" column indicates if the QTL is located in a high or low region of recombination. "NbSNP50", "LogPvaMax50",

1135 "NbSNP600", "LogPvaMax600", "NbSNPGBS", "LogPvaMaxGBS" are the number of 1136 significant SNPs and the most significant $-log_{10}(Pval)$ within the QTL for each technology 1137 across all environments. The physical position ("PosMax"), the proportion of the variance 1138 explained ("R2_LDMax") and the effect ("EffectMax") of the most significant SNP within 1139 the QTL is shown. "NbDiffEnv" gives the number of different situations that detected the 1140 QTL.

1141

1142 Additional file 9 (.docx):

Figure S10: Examples of comparison of QTLs detection on Chromosome 1, 6 and 8 for the different traits. Local distribution of the $-log_{10}(p\text{-value})$ and linkage disequilibrium (bottom) corrected by the kinship (r^2k) of all SNPs with the strongest associated marker within the chosen QTL for the three technologies. Ticks on different x-axes show the marker density of the three technologies (red for the 50K, blue for the 600K and green for the GBS). The vertical red line spots the position of the SNP with the maximum $-log_{10}(p\text{-value})$ within the QTL.

1150

1151 Additional file 10 (.docx):

1152 Figure S11: Pleiotropy of QTLs between the traits. Number of QTLs specific and shared by

1153 the three traits across all environments. Note that several QTLs from one trait were sometimes

1154 included in a single QTL of another trait.

1155 Figure S12: Percentage of stable QTLs across environments for the three traits (DTA: male

- 1156 flowering time, plantHT: Plant Height, GY: Grain Yield).
- 1157 **Table S4:** Stability of QTL across environments. DTA: male flowering time, plantHT: plant
- 1158 height, GY: grain yield traits.

| 1159 | Table S5: Recombination rate and proportion of low and high recombination regions. |
|------|---|
| 1160 | Average recombination rate ("RecRate") and proportion of the physical ("Phys") and genetic |
| 1161 | ("Genetic) map in low ("LowRec", <0.5 cM / Mbp) and high ("HighRec", >0.5 cM / Mbp) |
| 1162 | recombination regions for each chromosomes. "Chr" indicates the chromosome. Physical and |
| 1163 | genetic size columns indicated the size of each chromosome in bp and cM, respectively. |
| 1164 | Figure S13: Percentage of QTLs located in high (darkgrey) and low (lightgrey) |
| 1165 | recombinogenic regions. (a) male flowering time, (b) plant height and (c) grain yield. |
| 1166 | |
| 1167 | Additional file 11 (.pdf): |
| 1168 | Table S6: Description of inbred lines. Variety and accession along with the breeders, seeds |
| 1169 | providers and genetic groups obtained using ADMIXTURE for K=4 (Stiff Stalk, Iodent, |
| 1170 | Lancaster, Other). |
| 1171 | |
| 1172 | Additional file 12 (.docx): |
| 1173 | Table S7: Narrow sense heritability (h^2) and variance components (V_g , genetic variance; V_e , |
| 1174 | residual variance). The heritability and variance components were estimated for all traits |
| 1175 | (grain yield, male flowering time and plant height) using the R package Heritability [1]. |
| 1176 | Figure S14: Linkage disequilibrium based approach to delineate a physical window around |
| 1177 | each SNP, examplified with chromosome 3. Linkage disequilibrium (LD) windows were |
| 1178 | defined per chromosome for each SNP based on physical LD extent in low recombinogenic |

1179 regions (left part) and based on genetic LD extent in high recombinogenic regions (right part).

1180 These LD windows were used (i) to group significant SNPs into QTLs when they overlapped,

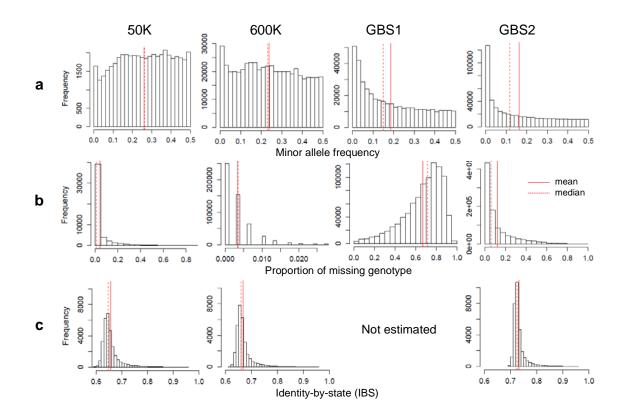
1181 (ii) to estimate genome coverage to detect QTLs by GWAS considering region not covered by

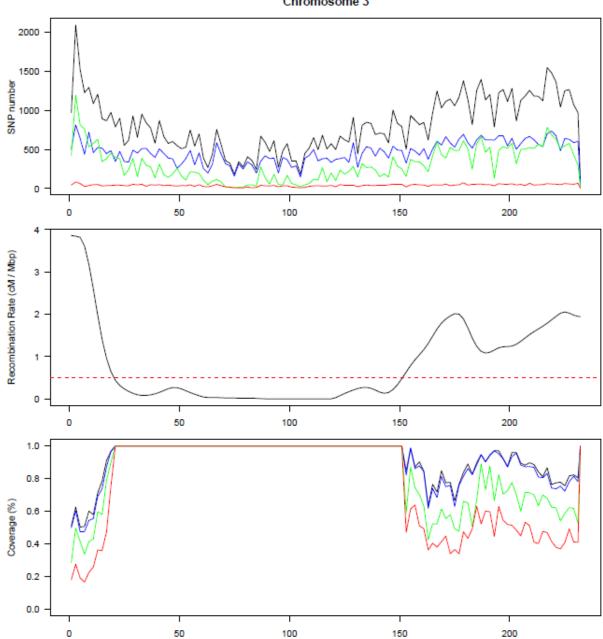
1182 LD windows, (iii) identify putative underlying genes involved in trait variations.

1183 **Figure S15:** QQ-plots representing observed $-log_{10}(p-value)$ against expected $-log_{10}(p-value)$ 1184 under null hypothesis (No association, black line). We tested association between 44,729 1185 SNPs from the 50K array and the male flowering time trait in one environment (Gai12R) 1186 using different GWAS models, kinship estimators and programs. (A) Comparisons between 1187 statistical models: M1 is the model without correction (green dots), M2 takes into account the 1188 group structure (blue dots), M3 takes into account kinship (IBD: K_freq) between individuals 1189 (purple dots) and M4 takes into account both group structure and kinship (red dots). (B) 1190 Comparison between mixed models using different estimates (IBS and IBD, K freq) of 1191 kinship. (C) Comparison of using or not Rincent *et al.* 2014 approach (using $K_{-}Chr$ vs 1192 K_{freq}). (D) Comparison between different informatics tools (EMMAX, ASReml, FasST-1193 LMM) that perform GWAS. 1194 Figure S16: Correlations between the GWAS results from the GBS genetic data using a 1195 kinship estimated from the PANZEA 50K array (x-axis) and a kinship estimated from the

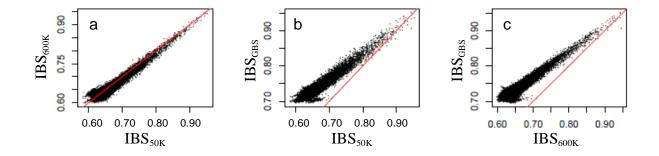
1196 GBS (y-axis). The horizontal and vertical lines are the threshold $-log_{10}(p-value) = 5$. The

- 1197 correlations were done using the flowering time (DTA) and plant height (plantHT) traits and
- 1198 the two sites, two years and two treatments (Gai12R, Gai12W, Gai13R, Gai13W, Ner12R,
- 1199 Ner12W, Ner13R, Ner13W).





Chromosome 3



bioRxiv preprint first posted online Nov. 23, 2018; doi: http://dx.doi.org/10.1101/476598. The copyright holder for this preprint (which was not peer-reviewed) is the author/funder, who has granted bioRxiv a license to display the preprint in perpetuity. It is made available under a CC-BY-NC-ND 4.0 International license.

